Atmos. Chem. Phys. Discuss., 13, 5315–5364, 2013
www.atmos-chem-phys-discuss.net/13/5315/2013/
doi:10.5194/acpd-13-5315-2013

Atmospheric Chemistry and Physics Discussions

Optical, microphysical, mass and geometrical properties of aged volcanic particles observed over Athens, Greece, during the Eyjafjallajökull eruption in April 2010 through synergy of Raman lidar and sunphotometer measurements

P. Kokkalis[1], A. Papayannis[1], V. Amiridis[2], R. E. Mamouri[1,3], I. Veselovskii[4], A. Kolgotin[4], G. Tsaknakis[1], N. I. Kristiansen[5], A. Stohl[5], and L. Mona[6]

[1]National Technical University of Athens, Physics Department, Laser Remote Sensing Laboratory, 15780, Zografou, Greece
[2]Institute for Astronomy, Astrophysics, Space Applications and Remote Sensing, National Observatory of Athens, Athens, Greece
[3]Department of Civil Engineering and Geomatics, Cyprus University of Technology, Lemessos, Cyprus
[4]Physics Instrumentation Center of General Physics Institute, Troitsk, Moscow 142190, Russia
[5]Norwegian Institute for Air Research, Kjeller, Norway

[6]Consiglio Nazionale delle Ricerche – Istituto di Metodologie per l'Analisi Ambientale, C. da S. Loja, 85050 Tito Scalo, Potenza, Italy

Received: 30 December 2012 – Accepted: 11 February 2013 – Published: 25 February 2013

Correspondence to: A. Papayannis (apdlidar@central.ntua.gr)

Published by Copernicus Publications on behalf of the European Geosciences Union.

Abstract

Vertical profiles of the optical (extinction and backscatter coefficients, lidar ratio and Ångström exponent), microphysical (mean effective radius, mean refractive index, mean number concentration) and geometrical properties, as well as of the mass concentration of volcanic particles from the Eyjafjallajökull eruption were retrieved at selected heights over Athens, Greece using a multi-wavelength Raman lidar system and inversion models, during 21–24 April 2010. Additionally, Aerosol Robotic Network (AERONET) particulate columnar measurements indicated the presence of volcanic particles over our area. Simulations of the volcanic partilcles dispersion, done by the FLEXPART model, confirmed the presence of these particles over Athens. Our lidar data showed volcanic particles layers, in the form of filaments after 7-day transport from the source (approximately 4000 km away from our site) between from ground levels up to nearly 10 km. Over Athens the volcanic particles layers were found to be mixed with locally produced aerosols, inside the Planetary Boundary Layer (PBL). Mean hourly-averaged lidar signals indicated that the layer thickness of volcanic particles, ranged between 1.5 and 2.2 km. The corresponding aerosol optical depth (AOD) found to vary from 0.014 to 0.184 at 355 nm and from 0.017 up to 0.174 at 532 nm. Furthermore, the corresponding lidar ratios (LR) ranged between 59.7–79.6 sr (at 355 nm) and 43.9–88.3 sr (at 532 nm). Additionally, we calculated that the mean effective radius of the volcanic particles was 0.13–0.38 µm, while their refractive index ranged from $1.39+0.009i$ to $1.48+0.006i$. Finally, our data also allowed us to quantitatively compare, for the first time, the volcanic ash concentrations simulated by FLEXPART with those calculated by the inversion code LIRIC, using data sets derived from coincident lidar-AERONET measurements. In general, good agreement was found between simulations and observations, concerning not only the geometrical properties of the volcanic particles layers, but also the particles mass concentration, with a correlation coefficient of the order of 0.75.

ACPD
13, 5315–5364, 2013

1 Introduction

The eruption of the Eyjafjallajökull volcano in Iceland during April and May 2010 created unprecedented disruption to the European air traffic, costing the aviation industry an estimated 200 million € per day (Harris et al., 2012). Eyjafjallajökull (63°38′ N, 19°36′ W, 1666 m above sea level – a.s.l.) has produced four eruptions in the last 1500 yr. The eruption started on 14 April and ended around 19 May 2010 (Sanderson, 2010; Showstack, 2010; Stohl et al., 2011). The total mass of the volcanic particles emitted from this eruption, was estimated to be of the order of 11.9 ± 5.9 Tg (Stohl et al., 2011), while the injection heights were found to be often of the order of 6–7 km, reaching even heights of 9–10 km (Emeis et al., 2011; Kaminski et al., 2011; Stohl et al., 2011; Mona et al., 2012).

The Eyjafjallajökull eruption was followed by scientists using a plethora of instruments, starting from ground-based, airborne and space-borne platforms. Permanent ground networks (seismic, weather, global positioning systems – GPS, lighting, hydrological, and borehole strain meters) monitored the volcanic activity in near real time in Iceland. On the other hand, satellite imagery was used to identify the plume dispersion and transportation, while dedicated scientific research flights enabled in situ monitoring and characterization, in terms of the chemical composition of the volcanic particles (Ansmann et al., 2010, 2011; Flentje et al., 2010; Sanderson, 2010; Bukowiecki et al., 2011; Dacre et al., 2011; Gasteiger et al., 2011; Schumann et al., 2011; Carboni et al., 2012; Chazette et al., 2012; Devenish et al., 2012; Gross et al., 2012; Lettino et al., 2012; Matthias et al., 2012; Millington et al., 2012; Prata and Prata, 2012; Rauthe-Schöch et al., 2012; Schleicher et al., 2012; Webley et al., 2012; Winker et al., 2012).

At 01:15 Universal Time Constant (UTC) on 14 April 2010 the Eyjafjallajökull started, thus an eruption plume was first visible over the volcanic site during the morning hours of that day, which a few hours later reached heights of about 10–11 km a.s.l. (Stohl et al., 2011). These height levels remained for the following days, while between 21 and 22 April, the volcanic particles plume reached lower heights (below 3 km a.s.l.).

ACPD
13, 5315–5364, 2013

The European aviation authorities were continuously informed (every 3–6 h) by the London Volcanic Ash Advisory Center (VAAC), about the criticalness of the volcanic particles presence over the European air continent (Carn et al., 2008; Webster et al., 2012). These reports were mainly based on volcanic particles dispersal simulations provided by the United Kingdom (UK) Meteorological Office (MetOffice) forecasts. Additionally, other institutions provided forecasts of the ash/volcanic particles concentrations (Stohl et al., 2011; Kristiansen et al., 2012; O'Dowd et al., 2012) at specific height levels (i.e. 3 and 5 km height a.s.l.). In addition, shortly after the end of the eruption, the UK MetOffice in their VAAC function distinguished the volcanic particles load, regarding the concentration in three levels: low ($< 200\,\mu g\,m^{-3}$), medium (200 to $4000\,\mu g\,m^{-3}$) and high ($> 4000\,\mu g\,m^{-3}$). If the volcanic particles concentrations were lower than $100\,\mu g\,m^{-3}$, then aircraft flights were quite safe, according to aircraft engine manufacturers (Casadevall, 1993; Airbus Customer Services, 2002; Car et al., 2008).

However, except the in situ airborne measurements, few other techniques could provide exact volcanic particles concentrations aloft. One such technique that became very useful during the Eyjafjallajökull eruption is the laser remote sensing (lidar) technique, which is a very favorable tool for the direct monitoring of the vertical profile of the aerosol optical properties. Besides the aerosol optical properties, one can estimate the volcanic aerosol geometrical and microphysical properties, as well as the ash concentration (Ansmann et al., 2010, 2011, 2012; Gasteiger et al., 2011; Chazette et al., 2012; Papayannis et al., 2012). The lidar technique was employed throughout Europe in the frame of the EARLINET project (Bösenberg et al., 2003) to monitor the volcanic particles plume dispersion – in time and space – over the European continent (Ansmann et al., 2010; Emeis et al., 2011; Gasteiger et al., 2011; Ansmann et al., 2012; Gross et al., 2012; Mona et al., 2012; Papayannis et al., 2012; Pappalardo et al., 2012; Revuelta et al., 2012; Rolf et al., 2012; Trickl et al., 2012).

In this paper, the volcanic particles measurements performed at the EARLINET station of Athens during the period 21–24 April 2010 are presented. The instrumentation and methods used is described in Sect. 2 and our results for a selected case study

ACPD
13, 5315–5364, 2013

are presented and analyzed in Sect. 3. Finally, our summary and conclusions are presented in Sect. 4.

2 Instrumentation and methods

2.1 The Raman lidar system

In Athens, Greece (37.97° N, 23.79° E, 220 m a.s.l.), the lidar system EOLE, is operating since 2000 at the National Technical University of Athens (NTUA). The system is being used for the determination of the aerosol optical properties, both in the Planetary Boundary Layer (PBL) and in the adjacent free troposphere (FT). The system is based on a Quanta Ray Lab-170-10 pulsed Nd:YAG laser, emitting simultaneously at 355, 532 and 1064 nm, with a repetition rate of 10 Hz. The corresponding output energies per pulse are 280, 310 and 260 mJ (Kokkalis et al., 2012). The laser beams are horizontally polarized (> 90 %) at 532–1064 nm and vertically polarized (> 90 %) at 355 nm. The laser beam containing all three wavelengths is expanded by a Galilean telescope (x3), before being emitted in the atmosphere, thus its divergence remains lower than 0.17 mrad (at full width at half maximum – FWHM). The full overlap of the system is of the order of 0.7–1 km a.s.l. (or 0.48–0.78 km above ground level), according to the detected wavelength.

A 300 mm diameter Cassegrainian telescope (focal length $f = 600$ mm, field of view = 1.25 mrad at half angle) collects all elastically backscattered lidar signals (355-532-1064 nm), as well as those generated by the spontaneous Raman effect (by atmospheric N_2 at 387–607 nm and H_2O at 407 nm). A high grade all-fused silica optical fiber (numerical aperture = 0.22 ± 0.02, core diameter = 1.5 mm) is used to transfer the lidar signals to an advanced 6-wavelength spectrometer, which is equipped with achromatic collimating lenses, dichroic beam splitters, as well as doublets, eye pieces and interference filters (IFF) placed in front of the detectors (Photomultiplier tubes – PMTs at 355-387-407-532-607 nm and Avalanche Photo Diode – APD at 1064 nm).

ACPD
13, 5315–5364, 2013

The lidar signals detected at 355, 387, 532, 607 and 1064 nm were used to derive the aerosol backscatter (at 355, 532 and 1064 nm) and extinction (at 355 and 532 nm) coefficients, as well as the Ångström exponent (AE) profiles, while the 407 nm channel was used to derive the water vapor mixing ratio (Mamouri et al., 2007). The NTUA lidar system is a part of EARLINET (European AeRosol LIdar NETwork) (Bösenberg et al., 2003) and has been quality-assured in the framework of network's activities through direct inter-comparisons, both at hardware (Matthias et al., 2004a) and algorithm levels (Böckmann et al., 2004; Pappalardo et al., 2004).

In order to qualitatively retrieve aerosol optical properties with a lidar system, several techniques have to be combined. Thus, the Klett inversion technique (Klett, 1985), with the assumptions, of a reference height in an aerosol-free region (e.g. the upper troposphere) and a constant extinction-to-backscatter ratio (the so-called lidar ratio – LR) value, is used to retrieve the atmospheric profile of the aerosol backscatter coefficient (b_{aer}) at the wavelengths of interest. The retrieved b_{aer} values are having an average uncertainty (due to both statistical and systematic errors) of the order of 20–30 % (Bösenberg et al., 1997).

When using the Raman technique (Ansmann et al., 1992), the uncertainties associated with the retrieved a_{aer} and b_{aer} vertical profiles are mainly due to the presence of noise on the received lidar signal. In this case the systematic uncertainties are of the order of 5–15 % on the b_{aer} and of 10–25 % on the a_{aer} (Ansmann et al., 1992; Mattis et al., 2002). Thus, with the Raman technique, the vertical profile of the aerosol parameter LR, can be calculated and not assumed, with a corresponding systematic uncertainty of the order of 5–10 %.

2.2 The AERONET station

The sun photometric observations reported in this paper were performed with a ground-based CIMEL sun-sky radiometer (Holben et al., 1998), which is part of the Aerosol Robotic Network (AERONET) Global Network (http://aeronet.gsfc.nasa.gov). The instrument is located on the roof of the Research Center for Atmospheric Physics and

ACPD
13, 5315–5364, 2013

Climatology of the Academy of Athens (37.99° N, 23.78° E, 130 m a.s.l.). The site is located in the city center and 10 km from the sea. This sun-photometric station is operated by the Institute for Astronomy, Astrophysics, Space Applications and Remote Sensing of the National Observatory of Athens (NOA). The sky-sun photometer, CIMEL, is performing automatically radiometric measurements. More precisely, the instrument is measuring both direct solar irradiance and diffuse sky radiance at various zenith and azimuth levels, with a field of view of 1.2°. The direct solar irradiance measurements are scheduled to be performed approximately every 15 min, while the sky diffuse almucantar or principal plane scenarios, every 30 min. The majority of the instruments operating in the AERONET network are based in a common configuration, including thus the standard wavelength detected signals at 440, 675, 870, 940 and 1020 nm. The CIMEL data used in this study are level 2.0 and will provide information about the columnar AOD, AE, aerosol size distribution and aerosol microphysical properties (Holben et al., 1998). The AERONET data products along with the technical specifications and the uncertainties of the CIMEL instrument are given in detail in Holben et al. (1998). More specifically, the total uncertainty of the AOD and the AE is influenced by various instrumental, calibration, atmospheric and methodological factors; for an AERONET field instrument, the AOD uncertainty is $< \pm 0.01$ for wavelengths longer than 440 nm and $< \pm 0.02$ for UV wavelengths (Eck et al., 1999), or about 10 % for a nominal aerosol optical depth of 0.1. The uncertainty of the sky radiance data and the resulting aerosol size distributions are determined based on the calibration uncertainty that is assumed $< \pm 5$ % at all four wavelength channels (Holben et al., 1998).

2.3 FLEXPART dispersion model

To simulate the ash transport, we employed the widely used Lagrangian particle dispersion model FLEXPART (Stohl et al., 1998, 2005). The simulations are based on the initial release of a large number of virtual particles, following the mean winds with superimposed random motions representing turbulence and convection. The model takes into account also the particles physical processes such as, sedimentation, dry and wet

ACPD
13, 5315–5364, 2013

deposition. The meteorological fields used in this study as input in FLEXPART model are taken from the European Centre for Medium-Range Weather Forecasts (ECMWF) with a horizontal resolution of 0.18° × 0.18° and 91 vertical levels. The output resolution in the horizontal and vertical level was set to be 0.25° × 0.25° and 250 m, respectively, with the last to be consisted of 38 vertical levels.

The major assumption, which is the strength of the initially injected volcanic ash particles, was determined by an inversion algorithm (Stohl et al., 2011). The aforementioned algorithm uses satellite data in order to constrain the emissions of the ash that was modeled. In general the FLEXPART simulation follows the scenario that 21 million particles were released from the volcano. Those particles were categorized in 25 classes, depending on their diameter ranging between 0.25 and 250 µm. However, only volcanic particles linked with diameters up to 10 µm could reach the lidar stations in Europe after several days of advection, due to the fact that the larger ones mostly fall out by gravitational settling (Näslund and Thaning, 1991), especially close to the source. More information on FLEXPART can be found at http://transport.nilu.no/flexpart and the model results used here are described in detail in Stohl et al. (2011) with further evaluations provided by Kristiansen et al. (2012).

2.4 LIRIC aerosol inversion code

The LIRIC (LIdar-Radiometer Inversion Code) algorithm has been developed within ACTRIS (Aerosols, Clouds and Trace gases Research InfraStructure Network – www.actris.net) by the Institute of Physics in Minsk (Belarus) in collaboration with the Laboratoire d'Optique Atmosphérique, Lille (France). LIRIC calculates the fine and coarse particle concentration profiles, utilizing the backscattered lidar signals (at 355, 532 and 1064 nm) and the column averaged aerosol microphysical properties retrieved from the sun photometer. Moreover, if the cross-polarized measurement at 532 nm is provided, the algorithm has the capability to differentiate the coarse mode concentration into spherical and non-spherical components. For the aforementioned calculations the assumption is made that except for the concentration, all other particle properties are

ACPD
13, 5315–5364, 2013

constant along the atmospheric column and equal to the column-averaged values provided by the sun photometer. The retrieval is based on a maximum-likelihood estimation of the concentration profiles, so that the lidar signals are reproduced within their measurement uncertainty and the integral of the retrieved aerosol concentrations matches the total volume concentration of the fine and coarse modes derived from sun photometric measurements. Furthermore, in order to avoid any unphysical values, smoothing constrains are imposed on the retrieved concentration profiles. A detailed description of LIRIC can be found in Chaikovsky et al. (2004, 2012) and Tsekeri et al. (2013).

The aerosol concentrations retrieved by LIRIC are expressed in parts per billion volume (ppbv). For the conversion of ppbv to $\mu g\,m^{-3}$, a methodology introduced by Ansmann et al. (2011, 2012), is applied. In this method the following equation is used:

$$m_{f/c} = \rho_{f/c} \times \overline{\left(\frac{V_{f/c}}{AOD_{f/c}}\right)} \times b_{f/c} \times LR_{f/c} \quad (1)$$

The subscript "f/c" denote either the fine or coarse aerosol mode. Fine and coarse mode are assumed to be representative for sulfate and volcanic dust particles, respectively. The first term (ρ) is the particle density and for our case the values for fine and coarse particles were 1.5 and $2.6\,g\,cm^{-3}$, respectively (http://volcanoes.usgs.gov/ash/properties.html/density, Schumann et al., 2011; Bukowiecki et al., 2011). The second term ($V_{f/c}/AOD_{f/c}$) is the ratio of the columnar particle volume concentration by the AOD, retrieved by AERONET, for fine and coarse aerosol modes. The third term is the aerosol backscatter coefficient retrieved by LIRIC for the corresponding two aerosol modes. Finally, the LR term is the aerosol lidar ratio for both fine and coarse mode particles. Ansmann et al. (2011) have recently used the values of $LR_f = 60 \pm 20$ sr and $LR_c = 50 \pm 10$ sr for pure non-volcanic and volcanic particles, respectively.

Furthermore, the terms a_{aer} and b_{aer} are re-calculated from AERONET column averaged extinction and backscatter coefficients data (for fine and coarse mode particles)

ACPD
13, 5315–5364, 2013

multiplied by the corresponding particle concentrations $C_c(z)$:

$$a_{aer}(\lambda, z) = a_f(\lambda) \times C_f(z) + a_c(\lambda) \times C_c(z)$$
$$b_{aer}(\lambda, z) = b_f(\lambda) \times C_f(z) + b_c(\lambda) \times C_c(z) \quad (2)$$

2.5 Derivation of the aerosol microphysical properties using models

The measured vertical profiles of the a_{aer} and b_{aer} at multiple wavelengths can be converted to the profiles of the particle microphysical parameters by using the regularization technique (Müller et al., 1999; Veselovskii et al., 2002, 2009). However, the application of this multi-wavelength (MW) lidar technique to aerosol dust data meets certain obstacles. Usually, all current lidar algorithms treat aerosols as an ensemble of spherical particles. However, it is well established that backscattering by irregularly shaped particles is weaker than by spheres of equivalent volume. To overcome these problems Mishchenko et al. (1997) suggested to model the irregularly shaped particles with a mixture of polydisperse, randomly oriented spheroids and showed that mixture of such simplified particles can mimic the properties of natural non-spherical aerosols.

Similarly, Dubovik et al. (2006) included the spheroid model in the AERONET retrieval algorithm. The same concept was later adopted by Veselovskii et al. (2010) for the incorporation of a spheroid model into the lidar retrieval of dust particles physical properties: in this case aerosols are modeled as a mixture of spheres and randomly oriented spheroids with a size-independent shape distribution. This technique was further applied to derive bulk aerosol properties from multi-wavelength Raman lidar measurements (Veselovskii et al., 2012). The results of numerical simulations demonstrate that for 10 % uncertainty of input optical data (a_{aer} and b_{aer}), the particle volume density (N), number density concentration (NC), the effective radius (r_{eff}) and the real and imaginary part of the particles refractive index (m_R and m_I, respectively) can be estimated with accuracy better than 30 %. In this paper the aerosols microphysical properties (r_{eff}, NC, m_R, m_I) in the lower free troposphere, inside the volcanic particles layers, were retrieved using the hybrid regularization technique provided by Veselovskii et al. (2002), using as input the optical data obtained from our Raman MW lidar measurements.

ACPD
13, 5315–5364, 2013

3 Case study analysis: 20–24 April 2010

3.1 FLEXPART simulations of ash advection and geometrical characteristics over Greece

We will now present a case study analysis for the period 20–24 April, where volcanic particles were advected to Greece, and where no desert dust events were predicted to be present over Europe. Thus the aerosol transport from Iceland to Greece was not affected by the presence of dust particles, in contrast to the period of May 2010 over Europe, where the Eyjafjallajökull volcanic particles were mixed with dust particles and even reached Western Turkey, as discussed in Papayannis et al. (2012).

Volcanic particles ejected during the Eyjafjallajökull April 2010 eruption covered major parts of Central Europe (e.g. France, Germany, United Kingdom, and Switzerland) only about two days after the eruption onset (Ansmann et al., 2010; Emeis et al., 2011; Devenish et al., 2012), while Southern-South Eastern Europe was affected later according to FLEXPART dispersion model simulations and local studies (Mona et al., 2012; Papayannis). Figure 1 shows the FLEXPART total column concentrations (in $\mathrm{mg\,m^{-2}}$) of volcanic ash for the period between 20 April (00:00 UTC) and 24 April (00:00 UTC). More precisely, on 20 April (00:00 to 12:00 UTC) remainders of the volcanic ash ejected earlier still covered Central Europe (with total columnar concentrations up to 800–900 $\mathrm{mg\,m^{-2}}$) and Northern Italy, and slowly reached Eastern Europe, as well. On the following day (21 April, at 00:00 UTC), the volcanic cloud moved more clearly southeastward, with bulk total columnar concentrations ranging between 200 and 700–800 $\mathrm{mg\,m^{-2}}$ over the Balkan area. Later on the same day (at 12:00 UTC) and on 22 April (00:00 UTC) the ash cloud passed over Greece, where maximum columnar concentrations of the order of 200–400 $\mathrm{mg\,m^{-2}}$ were simulated. Finally, the event started to fade out during the following days, from 22 April (12:00 UTC) to 24 April (00:00 UTC), as very low concentrations ($< 50\ \mathrm{mg\,m^{-2}}$) were simulated over South Eastern Europe, Northern Africa and Cyprus. To summarize, according to the FLEXPART simulations, Greece was mainly affected by volcanic particles between 21

ACPD
13, 5315–5364, 2013

April (12:00 UTC) and 24 April (00:00 UTC), but traces of volcanic particles were simulated already on 20 April (between 00:00 and 12:00 UTC). This is also demonstrated in the time-height contours of volcanic particles concentration (in $\mu g\,m^{-3}$), simulated by FLEXPART over Athens (from 20 April, 00:00 UTC to 24 April, 00:00 UTC), as shown in Fig. 2. The volcanic particles first appeared over Athens, in the height range between 3 and 5.5 km on 20 April (around 12:00 UTC) but at quite low concentrations (lower than $100\,\mu g\,m^{-3}$). Later, on the following day (21 April), higher concentrations of volcanic particles appeared in the height range from 3.5 to 6 km (from 15:00 UTC up to around 21:00 UTC) with concentrations of the order of 100–400 $\mu g\,m^{-3}$. Later that night, the volcanic particles (having concentrations of the order of 50 $\mu g\,m^{-3}$) started to settle down, reaching ground (on 22 April, around 07:00 UTC), where they were mixed with urban haze and local pollution.

Moreover, the FLEXPART simulations over Athens were qualitatively compared with our ground-based lidar measurements, using the temporal evolution of the range-corrected (RCS) lidar signal, as shown in Fig. 3. According to lidar measurements, some thin aerosol layers (in the form of filaments-shown in light blue color) were first observed at 10 km height around 16:00 UTC on 21 April, a situation similar to that reported also by Mona et al. (2012) over Southern Italy. During that night and until 04:00 UTC on 22 April, a new arrival of volcanic particles at around 4.5 km was observed. Additional aerosol layers (shown again in light blue color) were observed around 3.3 km and 2 km height (21 April at 15:00 UTC) and finally descended into the PBL around 16:00 UTC, where the volcanic particles were mixed with locally produced aerosols (shown in red color, from 21 April at 16:00 UTC to 23 April at around 04:00 UTC). However, some part of the aerosol layer observed around 3.3 km height, remained above the top of the PBL height (at around 3 km) during the following days (up to 23 April at 04:00 UTC), before the volcanic particles signal faded out at lower altitudes (around 1 km) on 24 April (around 03:00 UTC). A series of cirrus clouds were observed between 10 km and 12 km height (from 22 April around 18:00 UTC to 23 April around 04:00 UTC) that show up prominently in Fig. 3, but which are not related to volcanic particles. Later on 24 April

ACPD
13, 5315–5364, 2013

(around 00:00 UTC), these clouds also reached much lower heights, finally reaching 3 km.

Both aerosol layers depicted by the lidar in light blue color (from 10 km down to 5 km and around 3.5 km) were associated with pure volcanic particles dispersed over Athens, as we will show later. The height and time evolution of the lidar-depicted aerosol layers is almost identical to those simulated by FLEXPART (Fig. 2). Additionally, radiosonde measurements performed on 22 April (00:00 UTC) showed the existence of a very dry aerosol layer with relative humidity of 10 % (around 8.5 km), while it ranged from 20–50 % between 1 and 6 km, at heights where aerosols were observed by lidar at that time.

In order to validate the presence of volcanic particles in the free-troposphere, as observed by our lidar, we apply here the methodology developed by Mona et al. (2012) in the frame of the EARLINET-coordinated volcanic particles measurements (Pappalardo et al., 2012). To identify the presence of these particles Mona et al. (2012) used aerosol-related intensive parameters (e.g. extinction-related Ångström exponent – EAE and backscatter-related Ångström exponent – BAE) retrieved by MW Raman lidar measurements, in conjunction with air mass back trajectory analysis based on the HYbrid Single-Particle Lagrangian Integrated Trajectory (HYSPLIT) code.

However, prior to the aerosol "masking" procedure, an aerosol-cloud discrimination scheme is applied. The output results of the aerosol "masking" procedure are shown in Fig. 4 for 21 and 22 April. In this figure, the volcanic aerosol layers are denoted by different shades of grey color, according to the mean value of the aerosol backscatter coefficient at 532 nm. For the studied period, the PBL height was found to be below 2 km height. Therefore, from Fig. 4, we can see that on 21 April (17:00 UTC), free troposphere volcanic particles layers were observed from the top of the PBL up to 10–12 km height. During the afternoon hours of the same day, mixed aerosol types were detected in the height range from 2 to 4 km (denoted by magenta color). At the same heights, and during the early morning hours of April 22 (~ 01:00 UTC), the volcanic aerosols seem to present a maximum concentration above the top of the PBL (denoted by black

ACPD
13, 5315–5364, 2013

color), in terms of b_{aer}, which is of the order of 1 Mm^{-1} sr^{-1}. During the morning and noon hours of the same day, b_{aer} at 532 nm ranged from 0.1 to 1 Mm^{-1} sr^{-1}. According to HYSPLIT air mass back-trajectories and the Moderate Resolution Imaging Spectroradiometer (MODIS) satellite data (not shown), as well as the aerosol mask presented in Fig. 4, no dust, nor forest fires aerosols were present in the PBL of Athens, during these 2 days.

To further evaluate the FLEXPART model, in synergy with our lidar measurements, we performed data analysis schemes, regarding the volcanic aerosol layering and their concentration retrievals. Thus, our first qualitative comparison relies on the determination of the center of mass (CM) of the volcanic aerosol layers observed during the event studied, as detected by lidar and simulated by FLEXPART. Therefore, the CM height, z_c, for each layer has been calculated, following the definition given by Mona et al. (2006). More specifically, the height of the CM is estimated by the calculation of the backscatter weighted altitude (z_c) given as follows:

$$z_c = \frac{\int_{z_{bot}}^{z_{top}} z \times b_{aer} dz}{\int_{z_{bot}}^{z_{top}} b_{aer} dz} \quad (3)$$

The weighted, in terms of height, value of CM is a good approximation of the true aerosol CM, in case that both aerosol composition and size distribution are constant with height. Therefore, this approach is providing us with the valuable information of the altitude that the majority of the particles is located (Mona et al., 2006).

In Fig. 5 we present the temporal evolution of the CM height of the volcanic aerosol layers as (a) simulated by FLEXPART and (b) retrieved from the lidar measurements, for the period from 21 April 2010 (12:00 UTC) to 23 April 2010 (00:00 UTC), using hourly-averaged lidar data. The colored circles correspond to the volcanic ash concentration in the case of FLEXPART simulations and to the b_{aer} at 532 nm. For the latter,

ACPD
13, 5315–5364, 2013

we applied the Klett technique (Klett, 1985) using a LR equal to 60 sr. We have to note here that for the calculation of the CM values, we took into account even the lowest simulated ash concentrations (0.006 $\mu g\,m^{-3}$) (cf. Fig. 5a) and measured b_{aer} values ($1.5 \times 10^{-8}\,m^{-1}\,sr^{-1}$) (cf. Fig. 5b). Thus, in Fig. 5a and b, two clusters can be clearly found: volcanic aerosols detected in the upper troposphere (3–9 km a.s.l.) and in the lower troposphere (< 3 km a.s.l.). More precisely, the upper troposphere aerosols according to FLEXPART (and as will be shown later, they are mostly composed of coarse particles with r_{eff} around 0.37 µm) – traveled over central Europe and descended over our area. The lower troposphere aerosols are mostly linked to smaller particles (as will be shown in Fig. 14, where r_{eff} is around 0.13 µm), with NC about 5000 times greater than those in the upper troposphere. These small particles traveled – with low velocities – in lower troposphere, entering finally the PBL (~ 2 km) over Athens, thus mixing with local produced aerosols, such as urban haze and local pollution.

The same pattern of upper and lower troposphere volcanic aerosols was simulated by FLEXPART. For the studied time period the CM positions, detected by lidar and simulated by FLEXPART, were highly correlated, with a correlation coefficient (R^2) of the order of 0.89 (not shown). Actually, the difference between two pairs of CMs obtained, ranged from 0.11 to 2.2 km, with a mean relative difference of 0.5 km. Furthermore, it seems that FLEXPART simulated more efficiently (thus in better accordance with the lidar data) the higher aerosol layers (CM > 3 km) than the lower ones (CM < 3 km) (not shown). The correlation coefficient R^2 for CM > 3 km was 32.8 % higher than for CM < 3 km. Furthermore, by performing a Lag analysis (not shown) in these two datasets, practically no time delay was observed between the model predictions and the lidar observations.

In Fig. 6, we present the number of occurrences (cases) of the volcanic aerosol layer thickness, as predicted by FLEXPART (Fig. 6 – left hand side) and observed by lidar (Fig. 6 – right hand side), for all CM (a) and CM > 3 km (b). The dot corresponds to the position of the mean value of the aerosol layer thickness, while the error bars correspond to the standard deviation. Thus, for all the atmospheric column the FLEXPART

ACPD
13, 5315–5364, 2013

simulations showed a mean aerosol thickness of 1.92 ± 0.90 km, while the lidar observations gave a value of 1.16 ± 0.66 km. For layers with CM > 3 km, the FLEXPART simulations showed a mean aerosol layer thickness of 1.72 ± 0.87 km, while the lidar observations gave a value of 1.11 ± 0.71 km, which could be related to the coarser range resolution of the model output compared to the lidar data. The FLEXPART simulations revealed 32 cases with aerosol layer thickness between 1.35–1.77 km and 12 cases with aerosol layer thickness between 0.92–1.35 km. Based on the lidar observations, we found 25 cases with aerosol layer thickness between 0.82–1.17 km, and 19 cases with aerosol layer thickness between 0.48–0.82 km. Thus, we can say that the two patterns of volcanic particles transportation (in the upper and lower troposphere) were successfully simulated (in a qualitative manner) by FLEXPART, since the same patterns were detected by lidar, at the same height ranges and almost at the same time.

3.2 Volcanic particles concentrations

In order to further quantitatively evaluate the FLEXPART simulations regarding the volcanic particles concentrations, we used the LIRIC code (Tsekeri et al., 2013; Wagner et al., 2013). The methodology followed here is demonstrated with an example, using as input to LIRIC an hourly mean aerosol profile obtained by lidar (from 03:00–04:00 UTC) and the retrieved aerosol concentrations will be compared with the ones simulated by FLEXPART at 03:00 UTC.

We compared the retrieved b_{aer} profiles retrieved from the lidar measurements at 355, 532 and 1064 nm (assuming typical mean LR values of 75 sr at 355 nm, 65 sr at 532 nm and 60 sr at 1064 nm, as obtained from the previous night's Raman lidar measurements) with the LIRIC b_{aer} profiles retrieved at 355, 532 and 1064 nm. The LIRIC aerosol backscatter coefficient is calculated as the sum of the column-averaged fine and coarse particle backscatter coefficients from AERONET data, multiplied by the corresponding retrieved fine and coarse particle concentrations, as in Eq. (2). In Fig. 7 we present the b_{aer} profiles (along with their statistical error bars) calculated

ACPD
13, 5315–5364, 2013

by these two different methods at the three wavelengths and show that they revealed a quite good overall agreement. The observed differences, which are mostly due to the constant LR values assumed and used as input in the Klett technique, remain in general within the error bar limits, except at the lower 1.2–2 km height inside the PBL (only at 355 and 532 nm) where they are of the order of 40–50 %.

In order to determine the second term ($V_{f/c}/AOD_{f/c}$) of Eq. (1), we used the early morning AERONET observations (around 05:00 UTC), assuming that during the previous night the aerosol mixing remained stable and homogeneous. More specifically, the values that we calculated for $V_{f/c}/AOD_{f/c}$ were 0.6042 m^{-1} and 0.1535 m^{-1} for the aerosol coarse and fine mode, respectively. Those values are in very good agreement with the ones calculated in previous studies by Ansmann et al. (2011) and (2012).

Furthermore, in order to compare the aerosol concentration profiles, we degraded LIRIC's vertical spatial resolution (15 m) to the resolution used by FLEXPART (~ 250 m). Since FLEXPART has size-resolved information only for the ash aerosols, our comparison will be focused in the total (fine and coarse) mode retrieved by LIRIC. This is done mostly because LIRIC is based on AERONET's data and thus, the aerosol characterization regarding the diameter can be only up to 10 µm, while FLEXPART uses initial emissions with aerosols having a maximum diameter up to 250 µm, although there are too few with diameters greater than 10 µm.

In Fig. 8 we present the vertical profiles of the aerosol coarse and fine mode, as well as the total (fine and coarse mode) aerosol concentrations retrieved by LIRIC, compared to FLEXPART simulations. We can see that in general, the position of the volcanic ash layers are well predicted by FLEXPART compared to LIRIC for altitudes greater than 2 km, except of a relative vertical shift of about 0.5 km occurring between 2–4.5 km height. More specifically, the layers 2.0–2.5 km, 4.5–5.5 km, as well as 7.5–8.5 km were also detected by LIRIC. In the height range 1.5–2.5 km, a maximum relative difference of about 18 % was found, while in the 4.5–5.5 km range, the maximum relative difference was about 42 %.

ACPD
13, 5315–5364, 2013

The aforementioned analysis, concerning the retrieval of the aerosol concentrations using LIRIC, is applied in three consecutive and cloud-free lidar – AERONET data sets obtained at 03:00, 06:00 and 07:00 UTC on 22 April. Thus, in Fig. 9 we compare the volcanic aerosol concentration profiles, retrieved by LIRIC using lidar data (coarse and fine mode) and FLEXPART simulations for different times. In this figure we can see that for heights greater than 1.6 km, the mean aerosol concentration, retrieved by LIRIC for all three data sets, was found to be $10.86 \pm 4.16\,\mu g\,m^{-3}$, while it peaked up to $52.20\,\mu g\,m^{-3}$ around 2.1 km at 03:00 UTC; the simulated concentrations by FLEXPART gave a mean value of $8.83 \pm 0.73\,\mu g\,m^{-3}$ with a peaking value around $25.10\,\mu g\,m^{-3}$ around 2.35 km at 03:00 UTC. The coefficient R^2 between the FLEXPART and LIRIC profiles, ranged from 0.692 (at 03:00 UTC) to 0.837 (at 06:00 UTC), while it remained lower (0.743) at 07:00 UTC. Thus, from this comparison we can see that there is a quite good agreement between FLEXPART and LIRIC, for altitudes greater than 1.6 km. Below this height, we observed a large discrepancy between these two methods at 03:00 UTC (around 120 %), and much less at 07:00 UTC (around 50 %). This is due to the fact that FLEXPART simulates only ash particles and LIRIC uses as input lidar signals from all kind of mixed particles (volcanic and locally produced ones in the PBL of Athens).

3.3 Aerosol characteristics and comparison with other studies

In Fig. 10 (upper panel), we present the AERONET level 2.0 products for Athens, for the period between 20–24 April. In general, the presence of volcanic particles over Athens is not clearly depicted by the sunphotometric columnar measurements. More precisely, before the arrival of these particles over Athens, low AOD values at 500 nm (~ 0.1) were recorded on 20 April; on their arrival over Athens on 21 and 22 April, the AOD values picked to 0.25, a value very close to the ones reported for April 2010 over Lille (France) by Derimian et al. (2012) and for May 2010 over Athens by Papayannis et al. (2012). Once the event faded out the AOD values decreased again to 0.20. The respective fine mode particles, inside the atmospheric column, were of the order of

ACPD
13, 5315–5364, 2013

59.1–60.9 %, before and after the event, and remained around 76.8–78 %, during the event. This means that the fine mode particles dominated. Similarly, the corresponding AE values, retrieved from AOD values using the wavelength pair 440 nm/870 nm, were around 1.2 before and during the fading phase of the event, while they peaked to 1.6 during the event, showing again the presence of rather small particles, in contrast to values measured over Central Europe (Ansmann et al., 2010) where AE values were of the order of 0.35–0.4 during the volcanic eruption event. However, our findings for May 2010 (Papayannis et al., 2012) concerning AE values from AERONET data, for the days of pure volcanic particles presence over Athens, showed AE values ranging between 1 and 1.6, which are very close to the ones presented here during 21–24 April. In this period the total water vapor content remained close to 1.3 ± 0.2 cm. Moreover, the volcanic particles concentrations over Greece were quite low. For example, FLEXPART's ash column loadings over Central Europe a few days earlier forecasted values of the order of 600–1000 mg m^{-2} (Stohl et al., 2011), while in Greece, the maximum simulated ash loadings were 40–45 mg m^{-2} on 21 and 22 April (Fig. 1).

Moreover, the volcanic particles presence had a moderate signature on sunphotometric data over Athens, between 21 and 23 April, since the coarse mode AOD (as absolute value) increased by about 20 % during the event (Fig. 10, upper panel). This corresponds to an increase of the PM_{10} surface concentrations measured between 21 and 23 April (Fig. 10, lower panel), while the error bars correspond to the daily variability of the PM_{10} concentration. The PM_{10} concentration at the surface increased with a day of delay, which corresponds to the descent of the volcanic particles layer, as seen in both FLEXPART and lidar data. It seems that the volcanic particles added approximately 5 ± 0.1 µg m^{-3} to the PM_{10} measured at the surface, after 20 April.

In order to further characterize the volcanic particles over Athens, in terms of optical properties, we analyzed our cloud-free Raman lidar measurements [based on the retrieval of two a_{aer} (at 355 and 532 nm) and three b_{aer} (at 355, 532 and 1064 nm) profiles] for two time-windows on 22 April (depicted also by the aerosol masking in Fig. 4): 01:30–03:00 UTC and 20:02–22:00 UTC. Firstly, we calculated the vertical

ACPD
13, 5315–5364, 2013

profiles (Fig. 11) of the aerosol optical properties, such as the α_{aer}, b_{aer}, LR, EAE and BAE values, at 355, 532 and 1064 nm, based on our Raman lidar data on April 22 between 01:30 and 03:00 UTC (upper graph) and between 20:02 and 22:00 UTC (lower graph). More precisely (Fig. 11 – upper graph), based on the α_{aer} and b_{aer} vertical profiles, the aerosol masking, and the FLEXPART simulations, the aerosol layers between 1–2.3 km, 2.5–3 km and 5–6 km are considered to be volcanic particles layers (denoted by grey stripes). Similarly, in Fig. 11 (lower graph) the aerosol layers from 1.8 to 3.2 km are considered to be volcanic particles layers.

By comparing the nighttime Raman measurements of 22 April (Fig. 11), we can see that the EAE values decreased from 1.75 (during 01:30–03:00 UTC) (Fig. 11, upper graph) to 0.81 (20:02–22:00 UTC) (Fig. 11, lower graph), leaving the coarser particles in the lower parts of the atmosphere (between 2 to 3 km). Additionally, between the two layers extending from 2 to 2.4 km and 2.5 to 3 km (20:02–22:00 UTC), a shift in the optical properties is observed. The LR values increased from 63.1 to 77.2 sr at 355 nm and from 72.8 to 88.3 sr at 532 nm. In addition, the EAE values decreased from 0.91 to 0.71. This variability in combination with the increasing value of the relative humidity (from 20 to 40 %) are leading to a scenario that the volcanic ash particles, coated with sulfate, were coagulated with water wapor (Lathem et al., 2011) during their transport and/or mixed with locally produced particles, resulting to bigger particles. The same pattern, increasing LR values with increasing relative humidity, is also reported by Mona et al. (2012).

In Table 1 we present the mean optical properties of the volcanic particles calculated within the identified aerosol layers for these two time windows: EAE (pair 355–532 nm), BAE (pairs 355–532 nm, 532–1064 nm), LR (at 355 and 532 nm) and AOD (at 355 and 532 nm) values. We see that the EAE values ranged between 0.66–1.79, the BAE values (532–1064 nm pair) ranged between 0.97–1.24 and the BAE values (355–532 nm pair) ranged mainly between 1.26–1.72. The LRs inside the volcanic plume, at 355 nm, ranged between 59.7 and 79.6 sr, while at 532 nm, ranged between 43.9 and 88.3 sr. These values are very similar to those reported for Germany (Gross et al., 2012 on

ACPD
13, 5315–5364, 2013

17 April at Maisach; Ansmann et al., 2010 in Leipzig) and for Italy (Mona et al., 2012 on 19–22 April in Potenza), as we will discuss later. Our findings for May 2010 (Papayannis et al., 2012) showed very similar values for LRs inside the volcanic layers. Additionally, based on the α_{aer} values measured by our lidar system inside the almost pure volcanic ash layer (between 5 and 6 km on 22 April from 01:30–03:00 UTC), the corresponding AOD values at 355 nm and 532 nm were 0.014 and 0.017, respectively, which are similar to those reported by Sicard et al. (2012) over the Iberian peninsula, but quite lower from those measured over Athens one month later (Papayannis et al., 2012).

In the following we compare (cf. Fig. 12) the main volcanic aerosol optical properties, as measured by three EARLINET stations from 17 to 23 April over Maisach, Germany (Gross et al., 2011), Potenza, Italy (Mona et al., 2012) and Athens, Greece (present study). We can see in this figure that over Maisach, inside the volcanic particles layers, the mean particle depolarization ratio (denoted by open dots) was found to be nearly wavelength independent: 0.35 (at 355 nm) and 0.36 (at 532 nm). The LR values were found to be 55 ± 5 sr (at 355 nm) and 50 ± 5 sr (at 532 nm). Three days later (on 20 April), the observations performed in Italy by Mona et al. (2012), showed that the LR values at 355 nm, inside the volcanic particles layer, had remained of the same order ($\sim 54 \pm 13$ sr), while on the following day (on 21 April) they strongly decreased to around 40 ± 5 sr, compared to the ones measured over Maisach; additionally, the LR at 532 nm over Italy was of the same order as over Maisach. On the other hand, the mean particle depolarization ratio at 532 nm, dropped to lower values (0.15–0.23) compared to the ones measured over Maisach (0.35–0.36). Later, at the end of 22 April, the mean particle depolarization values increased back to 0.25 (at 532 nm), as the LR values were 78 and 80 sr (at 532 and 355 nm, respectively). Finally, over Athens, on the 22 April (01:30–03:00 UTC), the LR values were 75–80 sr (between 1 and 3 km) and around 60 sr (between 5 and 6 km). Later on that day (20:00–22:00 UTC), the LRs inside the volcanic plume, at 355 nm, ranged between 60 and 80 sr, while at 532 nm, ranged between 44 and 88.3 sr.

ACPD
13, 5315–5364, 2013

Generally, it seems that the optical and chemical properties of the volcanic aerosols were modified during their transport from the source region to our site, showing a decreasing trend in particle depolarization ratio, in combination with an increasing trend in the EAE and BAE values. This scenario shows that the volcanic plume was at first mostly composed of highly non-spherical coarse particles, which during their journey (aging) to our site either were removed by dry and/or wet deposition, or mixed with other particles (haze or urban), leading to more spherical and smaller particles. This is corroborated by an air mass back-trajectory analysis based on the FLEXPART model (see also Fig. 1) indicating that the aerosol-rich air masses sampled between 1.5 and 3 km height, had stagnated over Central Europe four days before our observations, where they were enriched with polluted and small anthropogenic particles of industrial and urban origin.

To further corroborate this scenario, we present in Fig. 13 the aerosol columnar sphericity (Dubovic et al., 2006) values obtained from three different AERONET stations in Europe (Leipzig, Potenza and Athens). A couple of days after the volcanic eruption onset, from 16 up to 19 April, the majority of the columnar sphericity values over Leipzig (denoted by black crosses) was below 35 % (although in some cases nearly spherical particles existed as well, with sphericities between 60–99 %) indicating that the atmosphere over that site was dominated mostly by non-spherical particles. Over Potenza on 21 April (denoted by blue circles) the majority of the columnar sphericity values showed increased values up to 58 %, while over Athens (denoted by triangles) most of the particles became even more spherical, with sphericity values of the order of 75–99 %. As discussed before, the increasing sphericity of the volcanic aerosols is probably linked to both mixing with water vapor and locally produced anthropogenic particles, especially in a city like Athens.

In Fig. 14 we present the main aerosol microphysical properties (r_{eff}, m_{R}, m_{I}) together with the NC values, as retrieved from lidar signal inversion techniques (see Sect. 2.5) for the five aerosol layers shown in Table 1. More precisely, during the early hours of 22 April (01:30–03:00 UTC), we see that in the two layers below 3 km height

ACPD
13, 5315–5364, 2013

we had the presence of rather small particles with r_{eff} below 0.13 µm, but in high concentrations (NC > 4000 particles cm^{-3}) (Fig. 14a, left graph). Moreover, these particles showed quite high absorption (m_I values were of the order of 0.006–0.010) with m_R values ranging between 1.38–1.39 (Fig. 14a, right graph). At higher altitudes (around 5.5 km height) NC dropped to very low values (NC ~ 20 particles cm^{-3}) but their r_{eff} values increased to around 0.38 µm. On the other hand, they showed quite low absorption (m_I values were of the order of 0.006) and a mean m_R value of 1.49. During the nighttime measurements of the same day (20:00–22:00 UTC) NC (Fig. 14b, left graph) decreased below 3 km height, to less than 700 particles cm^{-3}, but their mean effective radius increased to about 0.20–0.24 µm. On the other hand, they showed a lower absorption (m_I values were of the order of 0.003), while the m_R values were 1.57 at 2.2 km and 1.47 at 2.8 km height (Fig. 14b, right graph). Our r_{eff} values were much lower than those retrieved over Germany (Ansmann et al., 2010; Gasteiger et al., 2011; Weber et al., 2012) and France (Derimian et al., 2012), as these countries are much closer to the volcanic source region of Eyjafjallajökull than Greece, thus bigger particles stay near to their source due to gravitational settling.

4 Summary and conclusions

In this paper we presented the vertical profiles of the optical (a_{aer} and b_{aer}, LR, EAE and BAE), microphysical (mean r_{eff}, mean m_R and m_I, mean NC) and geometrical (layer thickness and aerosol center of mass) properties, as well as of the mass concentration of volcanic particles from the Eyjafjallajökull eruption, as retrieved for selected heights using a multi-wavelength Raman lidar system and inverse models, during the first days of the arrival of the volcanic particles over Athens, Greece in 21–24 April 2010. The days of 21 and 22 April were characterized by the maximum presence of volcanic particles over Athens, with high fine mode fractions in the total AOD (76.8 % and 78.0 %, respectively) and quite high AE values (of the order of 1.6) using collocated AERONET measurements (level 2.0 data) and aerosol masking schemes. Additionally,

ACPD
13, 5315–5364, 2013

high columnar ash concentrations (around 0.045 g m^{-2}) were simulated by FLEXPART. The highest maximum AOD value (~ 0.25 at 500 nm) was measured on 22 April, which was very similar to our volcanic particles observations in 12 May 2010 (Papayannis et al., 2012).

During the studied period, continuous lidar measurements were performed and revealed the presence of upper and low-mid tropospheric volcanic aerosols. Lofted volcanic particles layers, at about 10 km height, showed a downward motion during late afternoon hours on 21 April, similarly to observations reported for the same period by Mona et al. (2012). On the early hours of the following day (01:30–03:00 UTC) three distinct volcanic particles layers (between 1 and 6 km height) were identified and characterized in terms of their optical, microphysical and geometrical properties. The mean AOD value inside the volcanic particles layers was rather low, 0.090 (ranging from 0.014 to 0.184) at 355 nm and 0.074 (ranging from 0.017 to 0.174) at 532 nm. The corresponding values for LR ranged from 59.7 to 79.6 (mean value 72.4) at 355 nm and from 43.9 to 76.9 (mean value 65.4) at 532 nm. For the second time window of 22 April (20:02–22:00 UTC), two distinct volcanic particles layers were identified (between 2 and 3 km height). The mean AOD value inside these layers was rather low, 0.063 (ranging from 0.035 to 0.090) at 355 nm and 0.045 (ranging from 0.026 to 0.064) at 532 nm. The corresponding values for LR ranged from 63.3 to 77.2 (mean value 70.25) at 355 nm and from 72.8 to 88.3 (mean value 80.55) at 532 nm. For the volcanic particles layers below 3 km height, the respective EAE value (355 nm/532 nm) ranged from 0.66 to 1.79.

The main differences from the measurements performed in May 2010 over Athens (Papayannis et al., 2012), are mostly focusing on the greater heights where particles were observed in April (10 km on April versus 6 km on May), as well as that during April volcanic particles were mixed with locally produced ones in the lower troposphere, while in May they were mixed with advected dust particles.

The retrieval of the volcanic particles microphysical properties showed that the size of the lofted aerosols increased with height, as the mean r_{eff} value of the volcanic

ACPD
13, 5315–5364, 2013

particles, for both time windows, ranged from 0.13 to 0.38 µm. The m_R value of the volcanic particles ranged from 1.37 to 1.57, while m_I ranged from 0.003 to 0.006, indicating slight absorption by these particles. In contrast to lidar observations in Northern and Central Europe that detected optically thick lofted non-spherical volcanic particles, most of the volcanic particles that reached Athens, finally reached the lower troposphere, penetrated the PBL and became more spherical, as it was mixed with locally produced anthropogenic aerosols. Finally, we compared for the first time, the volcanic particles concentrations simulated by FLEXPART with those calculated by LIRIC for three time coincident lidar-AERONET datasets. This comparison was proved to be quite successful mostly above the PBL height (between 2.5 and 5.5 km height, with R^2 values close to 0.75.

Acknowledgements. This research has been co-financed by the European Union (European Social Fund – ESF) and Greek national funds through the Operational Program "Education and Lifelong Learning" of the National Strategic Reference Framework (NSRF) – Research Funding Program: Heracleitus II – Investing in knowledge society through the European Social Fund. AP, REM, VA and GT acknowledge that the research leading to these results has received also funding from the European Union Seventh Framework Programme (FP7/2007–2013) under grant agreement no. 262254 (ACTRIS).

References

Airbus Customer Services: Getting to grips with aircraft performance, Tech. Rep., Airbus S.A.S., Blagnac, France, 2002.

Ansmann A., Riebesell, M., Wandinger, U., Weitkamp, C., Voss, E., Lahmann, W., and Michaelis, W.: combined Raman elastic-backscatter lidar for vertical profiling of moisture, aerosol extinction, backscatter, and lidar ratio, Appl. Phys., B55, 18–28, 1992.

Ansmann, A., Tesche, M., Groß, S., Freudenthaler, V., Seifert, P., Hiebsch, A., Schmidt, J., Wandinger, U., Mattis, I., Müller, D., and Wiegner, M.: The 16 April 2010 major volcanic ash plume over central Europe: EARLINET lidar and AERONET photometer observations at

Leipzig and Munich, Germany. Geophys. Res. Lett. 37, L13810, doi:10.1029/2010GL043809, 2010.
Ansmann, A., Tesche, M., Seifert, P., Groß, S., Freudenthaler, V., Apituley, A., Wilson, K. M., Serikov, I., Linné, H., Heinold, B., Hiebsch, A., Schnell, F., Schmidt, J., Mattis, I., Wandinger, U., and Wiegner, M.: Ash and fine mode particle mass profiles from EARLINET-AERONET observations over central Europe after the eruptions of the Eyjafjallajökull volcano in 2010, J. Geophys. Res., 116, D00U02, doi:10.1029/2010JD015567, 2011.
Ansmann, A., Seifert, P., Tesche, M., and Wandinger, U.: Profiling of fine and coarse particle mass: case studies of Saharan dust and Eyjafjallajökull/Grimsvötn volcanic plumes, Atmos. Chem. Phys., 12, 9399–9415, doi:10.5194/acp-12-9399-2012, 2012.
Böckmann, C., Wandinger, U., Ansmann, A., Bösenberg, J., Amiridis, V., Boselli, A., Delaval, A., De Tomasi, F., Frioud, M., Grigorov, I., Hagard, A., Horvat, M., Iarlori, M., Komguem, L., Kreipl, S., Larcheveque, G., Matthias, V., Papayannis, A., Pappalardo, G., Rocadenbosch, F., Rodrigues, J. A., Schneider, J., Shcherbakov, V., and Wiegner, M.: Aerosol lidar intercomparison in the framework of the EARLINET project: Part II – Aerosol backscatter algorithms, Appl. Optics, 43, 977–989, 2004.
Bösenberg, J., Timm, R., and Wulfmeyer, V.: Study of retrieval algorithms for a backscatter lidar, Final Report, MPI Report No. 226, 1–66, Hamburg, 1997.
Bösenberg, J., Matthias, V., Amodeo, A., Amoiridis, V., Ansmann, A., Baldasano, J. M., Balin, I., Balis, D., Böckmann, C., Boselli, A., Carlsson, G., Chaikovsky, A., Chourdakis, G., Comeron, A., De Tomasi, F., Eixmann, R., Freudenthaler, V., Giehl, H., Grigorov, I., Hagard, A., Iarlori, M., Kirsche, A., Kolarov, G., Kolarev, L., Komguem, G., Kreipl, S., Kumpf, W., Larchevêque, G., Linné, H., Matthey, R., Mattis, I., Mekler, A., Mironova, I., Mitev, V., Mona, L., Müller, D., Music, S., Nickovic, S., Pandolfi, M., Papayannis, A., Pappalardo, G., Pelon, J., Pérez, C., Perrone, R. M., Persson, R., Resendes, D. P., Rizi, V., Rocadenbosch, F., Rodrigues, J. A., Sauvage, L., Schneidenbach, L., Schumacher, R., Shcherbakov, V., Simeonov, V., Sobolewski, P., Spinelli, N., Stachlewska, I., Stoyanov, D., Trickl, T., Tsaknakis, G., Vaμghan, G., Wandinger, U., Wang, X., Wiegner, M., Zavrtanik, M., and Zerefos, C.: EARLINET: A European Aerosol Research Lidar Network., MPI-Report, Max-Planck-Institut für Meteorologie, Hamburg, Germany, 348, 1–191, 2003.
Bukowiecki, N., Zieger, P., Weingartner, E., Jurányi, Z., Gysel, M., Neininger, B., Schneider, B., Hueglin, C., Ulrich, A., Wichser, A., Henne, S., Brunner, D., Kaegi, R., Schwikowski, M., Tobler, L., Wienhold, F. G., Engel, I., Buchmann, B., Peter, T., and Baltensperger,

ACPD
13, 5315–5364, 2013

U.: Ground-based and airborne in-situ measurements of the Eyjafjallajökull volcanic aerosol plume in Switzerland in spring 2010, Atmos. Chem. Phys., 11, 10011–10030, doi:10.5194/acp-11-10011-2011, 2011.

Carn, S., Krueger, A., Krotkov, N., Yang, K., and Evans, K.: Tracking volcanic sulfur dioxide clouds for aviation hazard mitigation, Nat. Hazards, 51, 325–343, doi:10.1007/s11069-008-9228-4, 2008.

Chaikovsky, A., Bril, A., Barun, V., Dubovik, O., Holben, B., and Thompson, A.: Studying altitude profiles of atmospheric aerosol parameters by combined multi-wavelength lidar and sun sky radiance measurements, Reviewed and revised papers presented at the 22nd International Laser Radar Conference, Matera, Italy, 345–348, 2004.

Chaikovsky, A., Dubovik, O., Goloub, P., Tanré, D., Pappalardo, G., Wandinger, U., Chaikovskaya, L., Denisov, S., Grudo, Y., Lopatsin, A., Karol, Y., Lapyonok, T., Korol, M., Osipenko, F., Savitski, D., Slesar, A., Apituley, A., Arboledas, L. A., Binietoglou, I., Kokkalis, P., Granados Muñoz, M. J., Papayannis, A., Perrone, M. R., Pietruczuk, A., Pisani, G., Rocadenbosch, F., Sicard, M., De Tomasi, F., Wagner, J., and Wang, X.: Algorithm and software for the retrieval of vertical aerosol properties using combined lidar/radiometer data: Dissemination in EARLINET, Reviewed and revised papers presented at the 26th International Laser Radar Conference, Porto Heli, Greece, 399–402, 2012.

Chazette, P., Dabas, A., Sanak, J., Lardier, M., and Royer, P.: French airborne lidar measurements for Eyjafjallajökull ash plume survey, Atmos. Chem. Phys., 12, 7059–7072, doi:10.5194/acp-12-7059-2012, 2012.

Dacre, H. F., Grant, A. L. M., Hogan, R. J., Belcher, S. E., ,Thomson, D. J., Devenish, B. J., Marenco, F., Hort, M. C., Haywood, J. M., Ansmann, A., Mattis, I., and Clarisse, L.: Evaluating the structure and magnitude of the ash plume during the initial phase of the 2010 Eyjafjallajökull eruption using lidar observations and NAME simulations, J. Geophys. Res., 116, D00U03, doi:10.1029/2011JD015608, 2011.

Derimian, Y., Dubovik, O., Tanré, D., Goloub, P., Lapyonok, T., and Mortier, A.: Optical properties and radiative forcing of the Eyjafjallajökull volcanic ash layer observed over Lille, France, in 2010, J. Geophys. Res., 117, D00U25, doi:10.1029/2011JD016815, 2012.

Devenish, B. J., Thomson, D. J., Marenco, F., Leadbetter, S. J., Ricketts, H., and Dacre, H. F.: A study of the arrival over the United Kingdom in April 2010 of the Eyjafjallajökull ash cloud using ground-based lidar and numerical simulations, Atmos. Environ., 148, 152–164, doi:10.1016/j.atmosenv.2011.06.033, 2012.

ACPD
13, 5315–5364, 2013

Dubovik, O., Sinyuk, A., Lapyonok, T., Holben, B. N., Mishenko, M., Yang, P., Eck, T. F., Volten, H., Munoz, O., Veihelmann, B., van der Zande, W. J., Leon, J.-F., Sorokin, M., and Slutsker, I.: Application of spheroid models to account for aerosol particle nonsphericity in remote sensing of desert dust, J. Geophys. Res., 111, D11208, doi:10.1029/2005JD006619, 2006.

Eck, T. F., Holben, B. N., Reid, J. S., Dubovik, O., Smirnov, A., O'Neill, N. T., Slutsker, I., and Kinne, S.: Wavelength dependence of the optical depth of biomass burning, urban, and desert dust aerosols, J. Geophys. Res., 104, 31333–31349, 1999.

Emeis, S., Forkel, R., Junkermann, W., Schäfer, K., Flentje, H., Gilge, S., Fricke, W., Wiegner, M., Freudenthaler, V., Groß, S., Ries, L., Meinhardt, F., Birmili, W., Münkel, C., Obleitner, F., and Suppan, P.: Measurement and simulation of the 16/17 April 2010 Eyjafjallajökull volcanic ash layer dispersion in the northern Alpine region, Atmos. Chem. Phys., 11, 2689–2701, doi:10.5194/acp-11-2689-2011, 2011.

Flentje, H., Claude, H., Elste, T., Gilge, S., Köhler, U., Plass-Dülmer, C., Steinbrecht, W., Thomas, W., Werner, A., and Fricke, W.: The Eyjafjallajökull eruption in April 2010 – detection of volcanic plume using in-situ measurements, ozone sondes and lidar-ceilometer profiles, Atmos. Chem. Phys., 10, 10085–10092, doi:10.5194/acp-10-10085-2010, 2010.

Gasteiger, J., Groß, S., Freudenthaler, V., and Wiegner, M.: Volcanic ash from Iceland over Munich: mass concentration retrieved from ground-based remote sensing measurements, Atmos. Chem. Phys., 11, 2209–2223, doi:10.5194/acp-11-2209-2011, 2011.

Gross, S., Freudenthaler, V., Wiegner, M., Gasteiger, J., Geiss, A., and Schnell, F.: Dual-wavelength linear depolarization ratio of volcanic aerosols: lidar measurements of the Eyjafjallajökull plume over Maisach, Germany, Atmos. Environ., 48, 85–96, 2012.

Harris, A. J. L., Gurioli, L., Hughes, E. E., and Lagreulet, S.: Impact of the Eyjafjallajökull ash cloud: A newspaper perspective, J. Geophys. Res., 117, B00C08, doi:10.1029/2011JB008735, 2012.

Holben, B. N., Eck, T. F., Slutsker, I., Tanré, D., Buis, J. P., Setzer, A., Vermote, E., Reagan, J. A., Kaufman, Y. J., Nakajima, T., Lavenu, F., Jankowiak, I., and Smirnov, A.: AERONET-A federated instrument network and data archive for aerosol characterization, Remote Sens. Environ., 66, 1–16, doi:10.1016/S0034-4257(98)00031-5, 1998.

Kaminski, E., Tait, S., Ferrucci F., Martet, M., Hirn, B., and Husson, P.: Estimation of ash injection in the atmosphere by basaltic volcanic plumes: the case of the Eyjafjallajökull 2010 eruption, J. Geophys. Res., 116, B00C02, doi:10.1029/2011JB008297, 2011.

ACPD
13, 5315–5364, 2013

Klett, J.: Lidar inversion with variable backscatter to extinction ratios, Appl. Optics, 24, 1638–1643, 1985.
Kokkalis, P., Papayannis, A., Mamouri, R. E., Tsaknakis, G., and Amiridis, V.: The EOLE lidar system of the National Technical University of Athens, Reviewed and revised papers presented at the 26th International Laser Radar Conference, 25–29 June 2012, Porto Heli, Greece, 629–632, 2012.
Kristiansen, N.I., Stohl, A., Prata, A. J., Bukowiecki, N., Dacre, H., Eckhardt, S., Henne, S., Hort, M. C., Johnson, B. T., Marenco, F., Neninger, B., Reitebuch, O., Seibert, P., Thomson, D. J.,Webster, H. N., and Weinzierl, B.: Performance assessment of a volcanic ash transport model mini-ensemble used for inverse modeling of the 2010 Eyjafjallajökull eruption, J. Geophys. Res., 117, D00U11, doi:10.1029/2011JD016844, 2012.
Lathem, T. L., Kumar, P., Nenes, A., Dufek, J., Sokolik, I. N., Trail, M., and Russell, A.: Hygroscopic properties of volcanic ash, Geophys. Res. Lett., 38, L11802, doi:10.1029/2011GL047298, 2011.
Lettino, A., Caggiano, R., Fiore, S., Macchiato, M., Sabia, S., and Trippetta, S.: Eyjafjallajökull volcanic ash in southern Italy, Atmos. Environ., 48, 97–103, doi:10.1016/j.atmosenv.2011.05.037, 2012.
Mamouri, R. E., Papayannis, A., and Tsaknakis, G.: First water vapor measurements over Athens, Greece, obtained by a combined Raman-elastic backscatter lidar system, Opt. Pura Appl., 41, 109–116, 2008.
Matthias, V., Freudenthaler, V., Amodeo, A., Balin, I., Balis, D., Bösenberg, J., Chaikovsky, A., Chourdakis, G., Comeron, A., Delaval, A., De Tomasi, F., Eixmann, R., Hågård, A., Komguem, L., Kreipl, S., Matthey, R., Vincenzo, R., Rodrigues, J. A., Wandinger, U., and Wang, X.: Aerosol lidar inter-comparison in the framework of the EARLINET project. 1. Instruments, Appl. Optics, 43, 961–976, 2004a.
Matthias, V., Balis, D., Bösenberg, J., Eixmann, R., Iarlori, M., Komguem, L., Mattis, I., Papayannis, A., Pappalardo, G., Perrone, M. R., and Wang, X.: Vertical aerosol distribution over Europe: Statistical analysis of Raman lidar data from 10 European Aerosol Research Lidar Network (EARLINET) stations, J. Geophys. Res., 109, D18201, doi:10.1029/2004JD004638, 2004b.
Matthias, V., Aulinger, A., Bieser, J., Cuesta, J., Geyer, B., Langmann, Bärbel, Serikov, I., Mattis, I., Minikin, A., Mona, L., Quante, M., Schumann, U., and Weinzierl, B.: The ash dispersion over Europe during the Eyjafjallajökull eruption – comparison of CMAQ

ACPD
13, 5315–5364, 2013

simulations to remote sensing and airborne in-situ observations, Atmos. Environ., 48, 184–194, doi:10.1016/j.atmosenv.2011.06.077, 2012.
Mattis, I., Ansmann, A., Müller, D., Wandinger, U., and Althausen, D.: Dual-wavelength Raman lidar observations of the extinction to-backscatter ratio of Saharan dust, Geophys. Res. Lett., 29, 1306, doi:10.1029/2002GL014721, 2002.
Millington, S. C., Saunders, R. W., Francis, P. N., and Webster, H. N.: Simulated volcanic ash imagery: A method to compare NAME ash concentration forecasts with SEVIRI imagery for the Eyjafjallajökull eruption in 2010, J. Geophys. Res., 117, D00U17, doi:10.1029/2011JD016770, 2012.
Mishchenko, M. I., Travis, L. D., Kahn, R. A., and West, R. A.: Modeling phase functions for dustlike tropospheric aerosols using a shape mixture of randomly oriented polydisperse spheroids, J. Geophys. Res., 102, 16831–16847, doi:10.1029/96JD02110, 1997.
Mona, L., Amodeo, A., Pandolfi, M., and Pappalardo, G.: Saharan dust intrusions in the Mediterranean area: three years of Raman lidar measurements, J. Geophys. Res., 111, D16203, doi:10.1029/2005JD006569, 2006.
Mona, L., Amodeo, A., D'Amico, G., Giunta, A., Madonna, F., and Pappalardo, G.: Multi-wavelength Raman lidar observations of the Eyjafjallajökull volcanic cloud over Potenza, southern Italy, Atmos. Chem. Phys., 12, 2229–2244, doi:10.5194/acp-12-2229-2012, 2012.
Müller, D., Wandinger, U., and Ansmann, A.: Microphysical particle parameters from extinction and backscatter lidar data by inversion with regularization: theory, Appl. Optics, 38, 2346–2357, 1999.
Näslund, E. and Thaning, L.: On the settling velocity in a non stationary atmosphere, Aerosol Sci. Technol., 14, 247–256, doi:10.1080/02786829108959487, 1991.
O'Dowd, C., Vargese, S., Martin, D., Flanagan, R., McKinstry, A., Ceburnis, D., Ovadnevaite, Martucci, G., Bialek, J., Monahan, C., Berresheim, H., Vaishya, A., Grigas, T., McGraw, Z., Jennings, S. G., Langmann, B., Semmler, T., and McGrath, R.: The Eyjafjallajökull ash plume – Part 2: Simulating ash cloud dispersion with REMOTE, Atmos. Environ., 48, 143–151, doi:10.1016/j.atmosenv.2011.10.037, 2012.
Papayannis, A., Mamouri, R. E., Amiridis, V., Giannakaki, E., Veselovskii, I., Kokkalis, Tsaknakis, G., Balis, D., Kristiansen, N. I., Stohl, A., Korenskiy, M., Allakhverdiev, K., Huseyinoglu, M. F., and Baykara, T.: Optical properties and vertical extension of ash layers over the Eastern Mediterranean as observed by Raman lidars during the Eyjafjallajökull eruption (May 2010), Atmos. Environ., 48, 56–65, 2012.

ACPD
13, 5315–5364, 2013

Pappalardo, G., Amodeo, A., Wandinger, U., Matthias, V., Bösenberg, J., Alpers, M., Amiridis, V., de Tomasi, F., Frioux, M., Iarlori, M., Komguen, L., Larcheveque, G., Papayannis, A., Schumacher, R., and Wang, X.: Aerosol lidar intercomparison in the frame of EARLINET: Part III: Aerosol extinction Raman lidar algorithm intercomparison, Appl. Optics, 43, 5370–5385, 2004.

Pappalardo, G., Mona, L., D'Amico, G., Wandinger, U., Adam, M., Amodeo, A., Ansmann, A., Apituley, A., Alados Arboledas, L., Balis, D., Boselli, A., Bravo-Aranda, J. A., Chaikovsky, A., Comeron, A., Cuesta, J., De Tomasi, F., Freudenthaler, V., Gausa, M., Giannakaki, E., Giehl, H., Giunta, A., Grigorov, I., Groß, S., Haeffelin, M., Hiebsch, A., Iarlori, M., Lange, D., Linné, H., Madonna, F., Mattis, I., Mamouri, R.-E., McAuliffe, M. A. P., Mitev, V., Molero, F., Navas-Guzman, F., Nicolae, D., Papayannis, A., Perrone, M. R., Pietras, C., Pietruczuk, A., Pisani, G., Preißler, J., Pujadas, M., Rizi, V., Ruth, A. A., Schmidt, J., Schnell, F., Seifert, P., Serikov, I., Sicard, M., Simeonov, V., Spinelli, N., Stebel, K., Tesche, M., Trickl, T., Wang, X., Wagner, F., Wiegner, M., and Wilson, K. M.: Four-dimensional distribution of the 2010 Eyjafjallajökull volcanic cloud over Europe observed by EARLINET, Atmos. Chem. Phys. Discuss., 12, 30203–30257, doi:10.5194/acpd-12-30203-2012, 2012.

Prata, A. J. and Prata, A. T.: Eyjafjallajökull volcanic ash concentrations determined using Spin Enhanced Visible and Infrared Imager measurements, J. Geophys. Res., 117, D00U23, doi:10.1029/2011JD016800, 2012.

Rauthe-Schöch, A., Weigelt, A., Hermann, M., Martinsson, B. G., Baker, A. K., Heue, K.-P., Brenninkmeijer, C. A. M., Zahn, A., Scharffe, D., Eckhardt, S., Stohl, A., and van Velthoven, P. F. J.: CARIBIC aircraft measurements of Eyjafjallajökull volcanic clouds in April/May 2010, Atmos. Chem. Phys., 12, 879–902, doi:10.5194/acp-12-879-2012, 2012.

Revuelta, M. A., Sastre, M., Fernández, A. J., Martín, L., García, R., Gómez-Moreno, F. J., Artíñano, B., Pujadas, M., and Molero, F.: Characterization of the Eyjafjallajökull volcanic plume over the Iberian Peninsula by lidar remote sensing and ground-level data collection, Atmos. Environ., 48, 46–55, doi:10.1016/j.atmosenv.2011.05.033, 2012.

Rolf, C., Krämer, M., Schiller, C., Hildebrandt, M., and Riese, M.: Lidar observation and model simulation of a volcanic-ash-induced cirrus cloud during the Eyjafjallajökull eruption, Atmos. Chem. Phys., 12, 10281–10294, doi:10.5194/acp-12-10281-2012, 2012.

Sanderson, K.: Out of the ashes, Nature, 465, 544–545, doi:10.1038/465544a, 2010.

Schleicher, N., Kramar, U., Dietze, V., Kaminski, U., and Norra, S.: Geochemical characterization of single atmospheric particles from the Eyjafjallajökull volcano eruption event

ACPD
13, 5315–5364, 2013

collected at ground-based sampling sites in Germany, Atmos. Environ., 48, 113–121, doi:10.1016/j.atmosenv.2011.05.034, 2012.
Schumann, U., Weinzierl, B., Reitebuch, O., Schlager, H., Minikin, A., Forster, C., Baumann, R., Sailer, T., Graf, K., Mannstein, H., Voigt, C., Rahm, S., Simmet, R., Scheibe, M., Lichtenstern, M., Stock, P., Rüba, H., Schäuble, D., Tafferner, A., Rautenhaus, M., Gerz, T., Ziereis, H., Krautstrunk, M., Mallaun, C., Gayet, J.-F., Lieke, K., Kandler, K., Ebert, M., Weinbruch, S., Stohl, A., Gasteiger, J., Groß, S., Freudenthaler, V., Wiegner, M., Ansmann, A., Tesche, M., Olafsson, H., and Sturm, K.: Airborne observations of the Eyjafjalla volcano ash cloud over Europe during air space closure in April and May 2010, Atmos. Chem. Phys., 11, 2245–2279, doi:10.5194/acp-11-2245-2011, 2011.
Showstack, R.: Eruptions of Eyjafjallajökull volcano, Iceland, EOS Trans. Am. Geophys. Union, 91, 190–191, doi:10.1029/2010EO210002, 2010.
Sicard, M., Guerrero-Rascado, J. L., Navas-Guzmán, F., Preißler, J., Molero, F., Tomás, S., Bravo-Aranda, J. A., Comerón, A., Rocadenbosch, F., Wagner, F., Pujadas, M., and Alados-Arboledas, L.: Monitoring of the Eyjafjallajökull volcanic aerosol plume over the Iberian Peninsula by means of four EARLINET lidar stations, Atmos. Chem. Phys., 12, 3115–3130, doi:10.5194/acp-12-3115-2012, 2012.
Stohl, A., Hittenberger, M., and Wotawa, G.: Validation of the Lagrangian particle dispersion model FLEXPART against large scale tracer experiment data, Atmos. Environ., 32, 4245–4264, 1998.
Stohl, A., Forster, C., Frank, A., Seibert, P., and Wotawa, G.: Technical note: The Lagrangian particle dispersion model FLEXPART version 6.2, Atmos. Chem. Phys., 5, 2461–2474, doi:10.5194/acp-5-2461-2005, 2005.
Stohl, A., Prata, A. J., Eckhardt, S., Clarisse, L., Durant, A., Henne, S., Kristiansen, N. I., Minikin, A., Schumann, U., Seibert, P., Stebel, K., Thomas, H. E., Thorsteinsson, T., Tørseth, K., and Weinzierl, B.: Determination of time- and height-resolved volcanic ash emissions and their use for quantitative ash dispersion modeling: the 2010 Eyjafjallajökull eruption, Atmos. Chem. Phys., 11, 4333–4351, doi:10.5194/acp-11-4333-2011, 2011.
Trickl, T., Giehl, H., Jäger, H., and Vogelmann, H.: 35 years of stratospheric aerosol measurements at Garmisch-Partenkirchen: from Fuego to Eyjafjallajökull, and beyond, Atmos. Chem. Phys. Discuss., 12, 23135–23193, doi:10.5194/acpd-12-23135-2012, 2012.
Tsekeri, A., Amiridis, V., Kokkalis, P., Basart, S., Chaikovsky, A., Dubovik, O., Mamouri, R. E., Papayannis, A., and Baldasano, J. M.: Application of synergetic lidar and sumphotometer

ACPD
13, 5315–5364, 2013

algorithm for the characterization of a dust event over Athens, Greece, Brit. J. Environ. Climate Change, in review, 2013.
Veselovskii, I., Kolgotin, A., Griaznov, V., Müller, D., Wandinger, U., and Whiteman, D. N.: Inversion with regularization for the retrieval of tropospheric aerosol parameters from multiwavelength lidar sounding, Appl. Optics, 41, 3685–3699, 2002.
Veselovskii, I., Whiteman, D. N., Kolgotin, A., Andrews, E., and Korenskii, M.: Demonstration of aerosol property profiling by multi-wavelength lidar under varying relative humidity conditions, J. Atmos. Ocean. Tech., 26, 1543–1557, 2009.
Veselovskii, I., Dubovik, O., Kolgotin, A., Lapyonok, T., Di Girolamo, P., Summa, D., Whiteman, D. N., Mishchenko, M., and Tanré, D.: Application of randomly oriented spheroids for retrieval of dust particle parameters from multi-wavelength lidar measurements, J. Geophys. Res., 115, D21203, doi:10.1029/2010JD014139, 2010.
Veselovskii, I., Dubovik, O., Kolgotin, A., Korenskiy, M., Whiteman, D. N., Allakhverdiev, K., and Huseyinoglu, F.: Linear estimation of particle bulk parameters from multi-wavelength lidar measurements, Atmos. Meas. Tech., 5, 1135–1145, doi:10.5194/amt-5-1135-2012, 2012.
Wagner, J., Ansmann, A., Wandinger, U., Seifert, P., Schwarz, A., Tesche, M., Chaikovsky, A., and Dubovik, O.: Evaluation of the Lidar/Radiometer Inversion Code (LIRIC) to determine microphysical properties of volcanic and desert dust, Atmos. Meas. Tech. Discuss., 6, 911–948, doi:10.5194/amtd-6-911-2013, 2013.
Weber, K., Eliasson, J., Vogel, A., Fischer, C., Pohl, T., van Haren, G., Meier, M., Grobety, B., and Dahmann, D.: Airborne in-situ investigations of the Eyjafjallajökull volcanic ash plume on Iceland and over borth-western Germany with light aircrafts and optical particle counters, Atmos. Environ., 48, 9–21, 2012.
Webley, P. W., Steensen, T., Stuefer, M., Grell, G., Freitas, S., and Pavolonis, M.: Analyzing the Eyjafjallajökull 2010 eruption using satellite remote sensing, lidar and WRF-Chem dispersion and tracking model, J. Geophys. Res., 117, D00U26, doi:10.1029/2011JD016817, 2012.
Webster, H. N., Thomson, D. J., Johnson, B. T., Heard, I. P. C., Turnbull, K. F., Marenco, F., Kristiansen, N. I., Dorsey, J. R., Minikin, A., Weinzierl, B., Schumann, U., Sparks, S. S. J., Loughlin S. C., Hort, M., Leadbetter, S. J., Devenish, B., Manning, A. J., Witham, C., Haywood, J. M., and Golding, B.: Operational prediction of ash concentrations in the distal volcanic cloud from the 2010 Eyjafjallajokull eruption, J. Geophys. Res., 117, D00U08, doi:10.1029/2011JD016790, 2012.

ACPD
13, 5315–5364, 2013

Winker, D. M., Liu, A., Omar, A., Tackett, J., and Fairlie, D.: CALIOP observations of the transport of ash from the Eyjafjallajökull volcano in April 2010, J. Geophys. Res., 117, D00U15, doi:10.1029/2011JD016499, 2012.

ACPD
13, 5315–5364, 2013

Table 1. Mean values and standard deviations of the aerosol extinction-related Ångström exponent (355 nm/532 nm), aerosol backscatter-related Ångström exponent (355 nm/532 nm and 532 nm/1064 nm), lidar ratio (at 355 and 532 nm), and aerosol optical depth at 355 and 532 nm, obtained by the Raman lidar over Athens, Greece, between 01:30 UTC and 03:00 UTC (upper graph) and 20:00 UTC and 22:00 UTC (lower graph).

ATHENS, NTUA LIDAR, 22 April 2010, 01:30–03:00 UTC								
	Height [m]	Aa(355/532)	Ab(355/532)	Ab(532/1064)	LR355	LR532	AOD355	AOD532
LAYER 1	1000–2300	1.69 ± 0.07	1.61 ± 0.02	1.17 ± 0.03	79.6 ± 0.5	76.9 ± 2.8	0.184	0.174
LAYER 2	2500–3000	1.79 ± 0.15	1.72 ± 0.06	1.24 ± 0.01	77.7 ± 1.2	75.6 ± 4.6	0.076	0.037
LAYER 3	5000–6000	0.66 ± 0.06	−0.3 ± 0.05	1.19 ± 0.04	59.7 ± 2.1	43.9 ± 8.1	0.014	0.017
ATHENS, NTUA LIDAR, 22 April 2010, 20:00–22:00 UTC								
	Height [m]	Aa(355/532)	Ab(355/532)	Ab(532/1064)	LR355	LR532	AOD355	AOD532
LAYER 1	2000–2400	0.91 ± 0.06	1.26 ± 0.02	0.98 ± 0.02	63.3 ± 0.8	72.8 ± 1.1	0.090	0.064
LAYER 2	2500–3000	0.71 ± 0.12	1.52 ± 0.12	0.97 ± 0.01	77.2 ± 7.0	88.3 ± 6.8	0.035	0.026

ACPD
13, 5315–5364, 2013

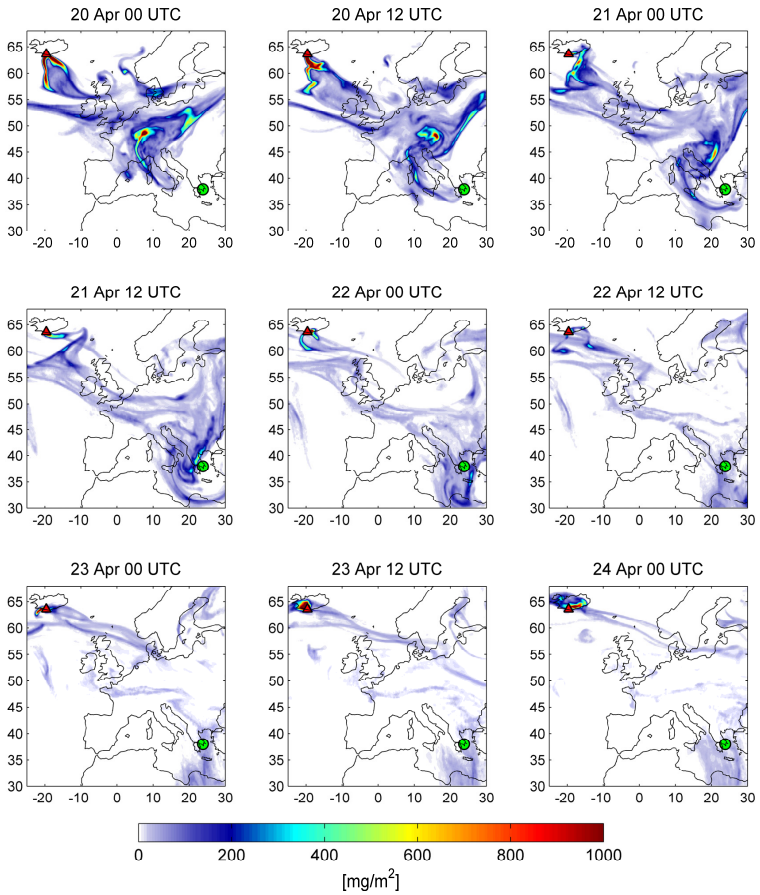

Fig. 1. FLEXPART simulations of the Eyjafjallajökull volcanic ash dispersion (total column in mg m^{-2} for all 25 particle size classes) for the period of 20 April 2010 (00:00 UTC) to 24 April 2010 (00:00 UTC). The position of the Athens lidar station is marked by a green circle, while the location of the volcano is shown by a red triangle.

ACPD
13, 5315–5364, 2013

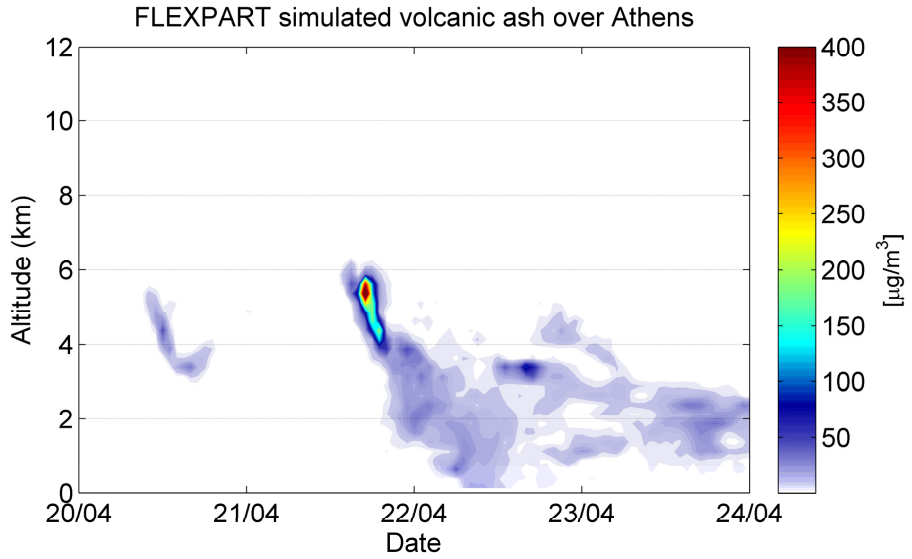

Fig. 2. Time-height contours of volcanic ash concentrations (in $\mu g\,m^{-3}$) over Athens from 20 April 2010 at 00:00 UTC to 24 April 2010 at 00:00 UTC, as simulated by FLEXPART.

ACPD
13, 5315–5364, 2013

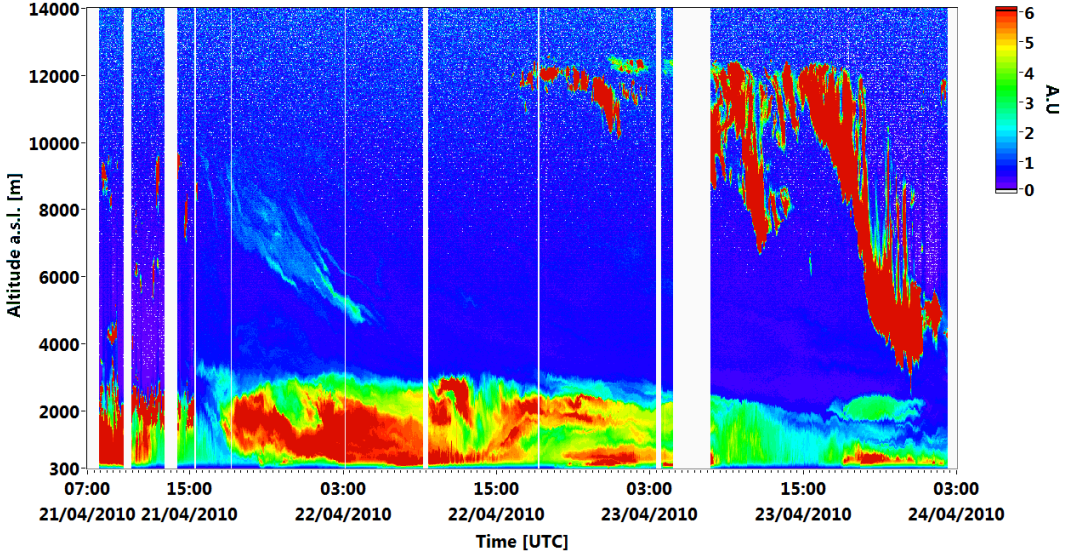

Fig. 3. Temporal evolution of the range-corrected lidar signal (RCS) in arbitrary units (A.U.) obtained over Athens at 1064 nm, between 21 April 2010 (07:00 UTC) and 24 April 2010 (03:00 UTC). All colored structures correspond to the presence of aerosols, except after 22 April 2010 (15:00 UTC) where clouds are detected at heights between 4 and 12.5 km.

ACPD
13, 5315–5364, 2013

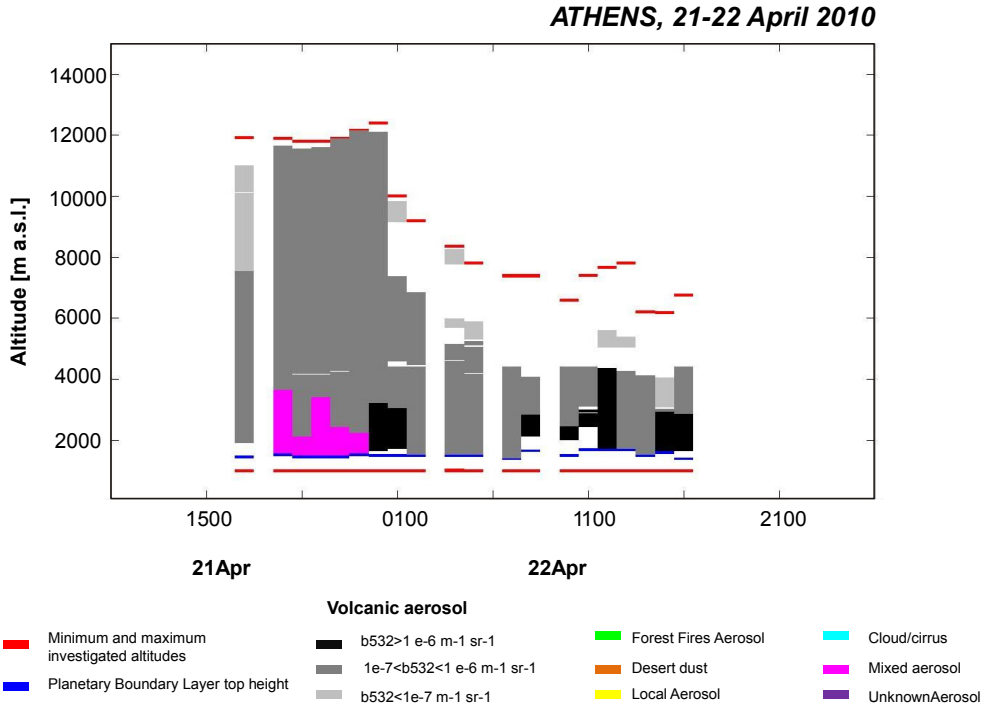

Fig. 4. Aerosol masking for the particle layers detected over Athens from 21 April 2010 (16:00 UTC) to 22 April 2010 (16:30 UTC).

ACPD
13, 5315–5364, 2013

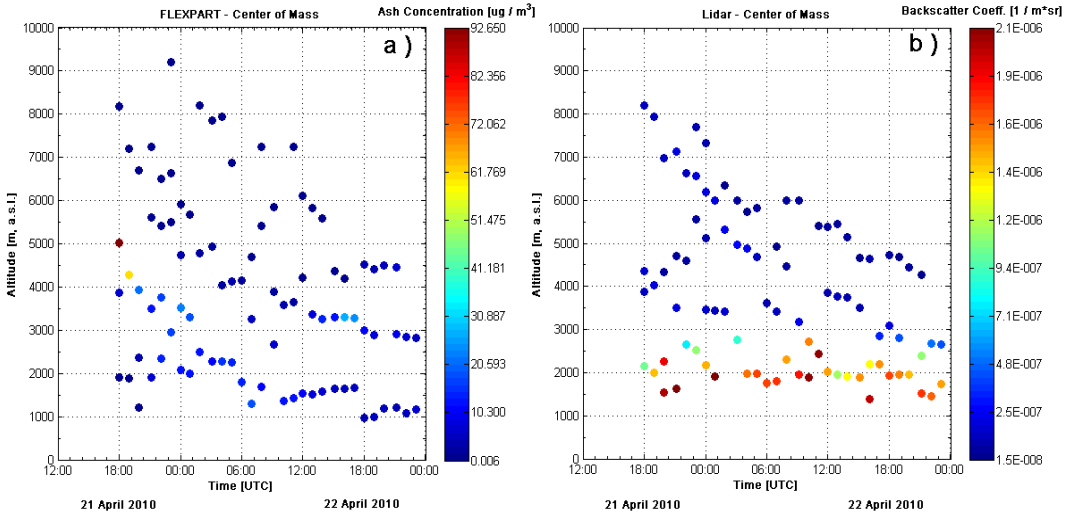

Fig. 5. Center of mass (CM) of the volcanic ash layers, as **(a)** simulated by FLEXPART according to the ash concentration (in $\mu g\,m^{-3}$) and **(b)** detected by Raman lidar measurements over Athens (hourly-averaged data) according to the aerosol backscatter coefficient (in $m^{-1}\,sr^{-1}$) at 532 nm, for the period: 21 April 2010 (12:00 UTC) and 23 April 2010 (00:00 UTC).

ACPD
13, 5315–5364, 2013

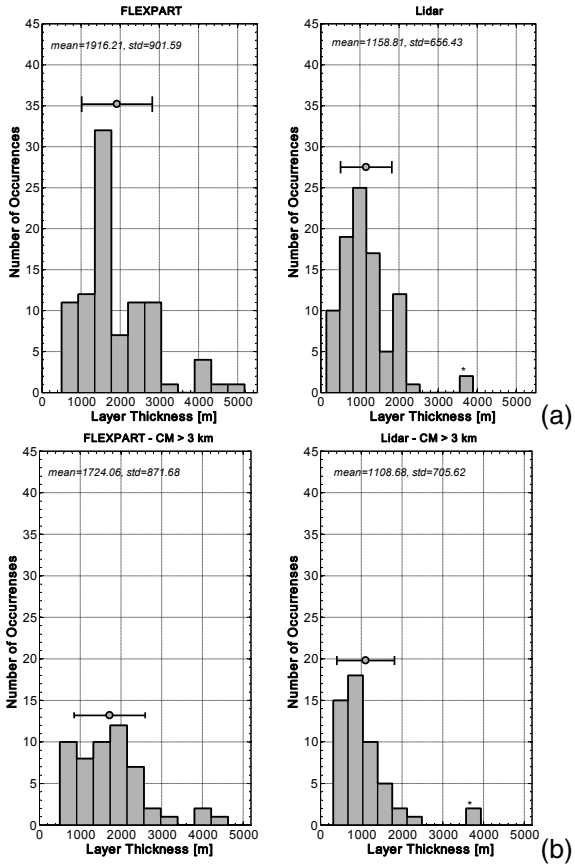

Fig. 6. Volcanic aerosol layer thickness (in m) distribution according to FLEXPART simulations (left) and Raman lidar measurements (right), **(a)** for the whole atmospheric column and **(b)** for a center of mass (CM) > 3 km height, for the period: 21 April 2010 (12:00 UTC) and 23 April 2010 (00:00 UTC), over Athens. The dot corresponds to the position of the mean value of the aerosol layer thickness, while the error bars correspond to the standard deviation.

ACPD
13, 5315–5364, 2013

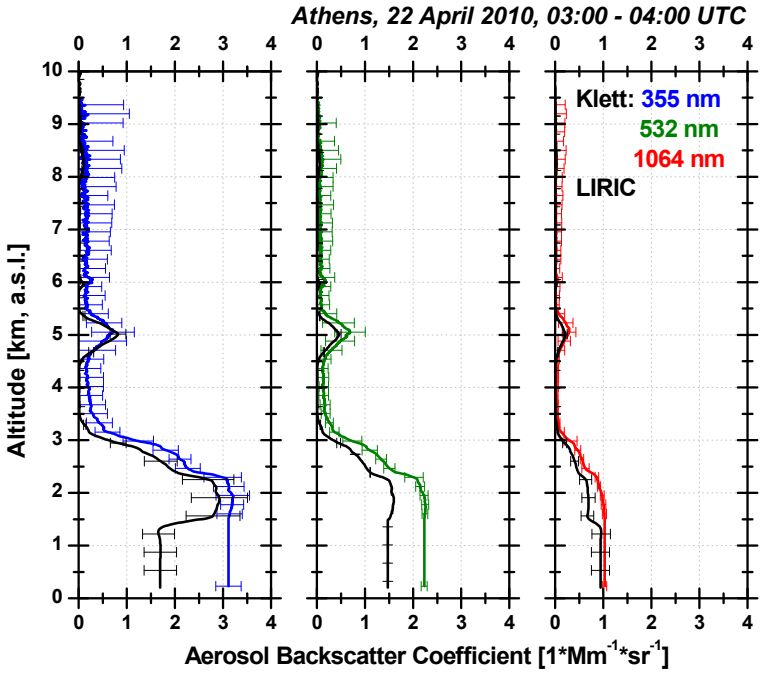

Fig. 7. Aerosol backscatter coefficient profiles (in $Mm^{-1}\ sr^{-1}$) calculated with two different methods: LIRIC (black line) and Klett technique at 355 (blue line), 532 (green line) and 1064 nm (red line), on 22 April 2010 (03:00–04:00 UTC) over Athens.

ACPD
13, 5315–5364, 2013

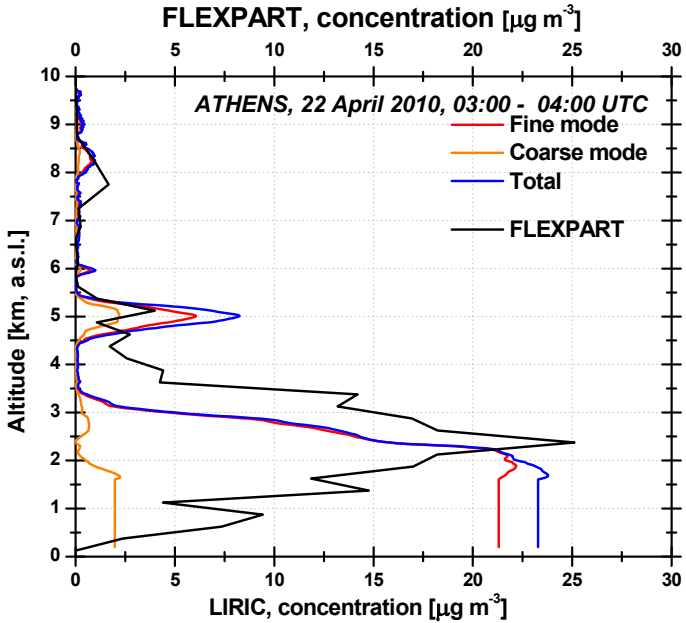

Fig. 8. Coarse mode, fine mode and total concentrations retrieved by LIRIC versus ash concentration (in $\mu g\,m^{-3}$) simulated by FLEXPART for 22 April 2010 (03:00 UTC) over Athens.

ACPD
13, 5315–5364, 2013

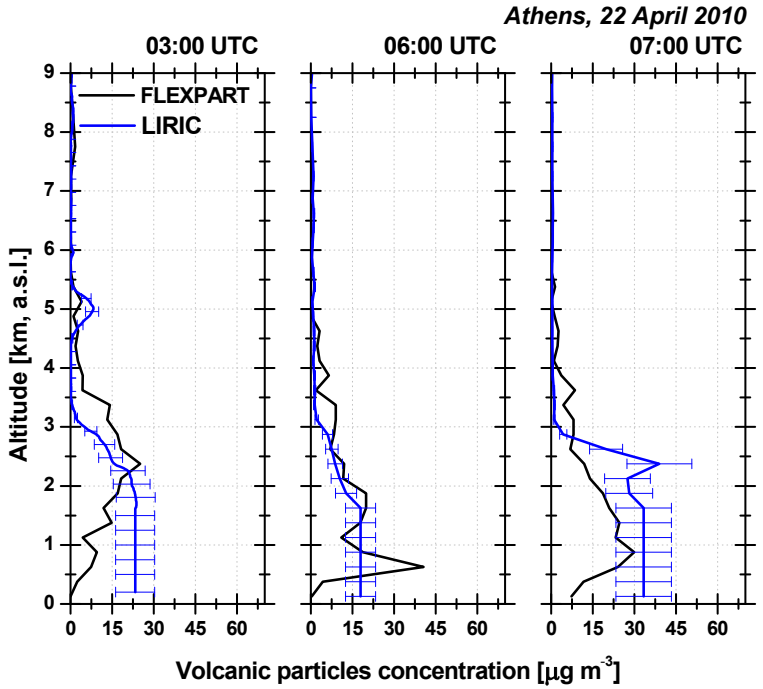

Fig. 9. Comparison of volcanic aerosol concentrations (in $\mu g\,cm^{-3}$) retrieved by LIRIC and simulated by FLEXPART on 22 April 2010 over Athens, at 03:00 UTC (left), 06:00 UTC (middle) and 07:00 UTC (right).

ACPD
13, 5315–5364, 2013

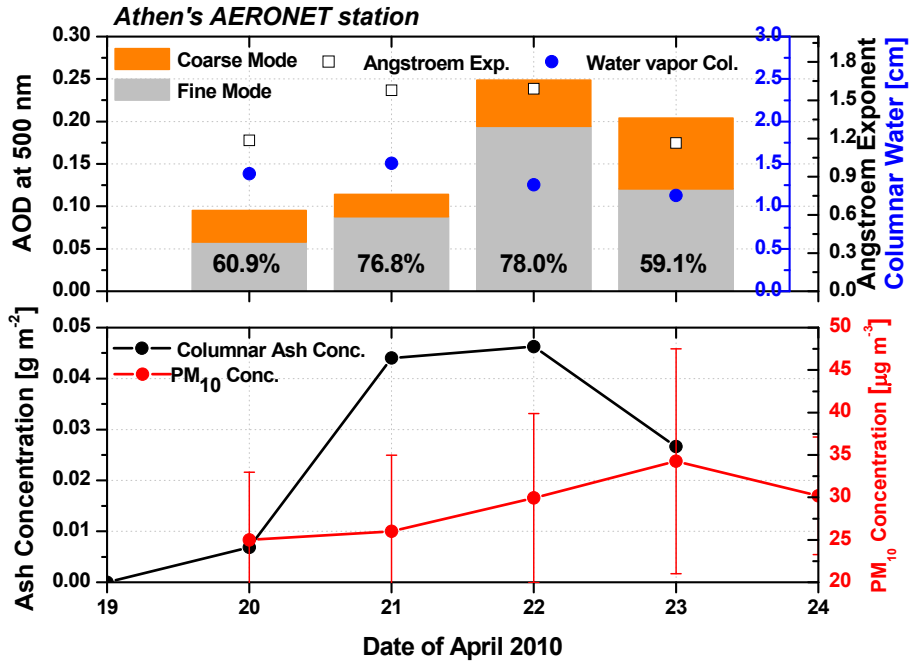

Fig. 10. AERONET fine/coarse mode Aerosol Optical Depth (AOD) obtained over Athens at 500 nm for the period between 19–24 April 2010, Ångström exponent of 440 nm/870 nm along with the columnar water vapor (cm) (upper panel). Temporal evolution of the volcanic ash columnar concentration (in g m^{-2}) according to FLEXPART simulations (black line) and of PM_{10} daily surface concentration (in μg m^{-3}) measured (red line) in situ (lower panel). The error bars correspond to the daily variability of the PM_{10} concentration.

ACPD
13, 5315–5364, 2013

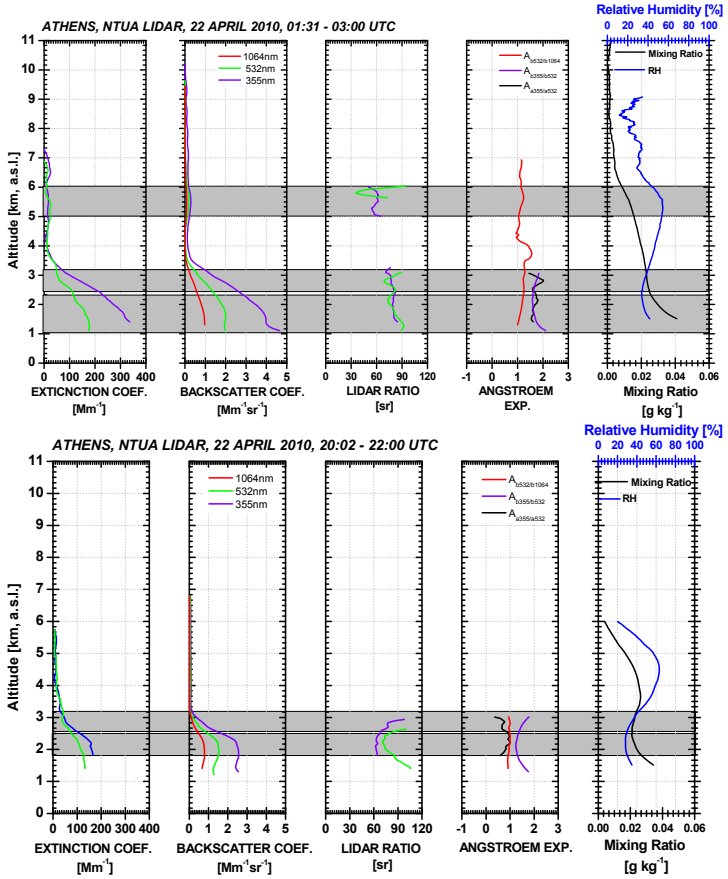

Fig. 11. Aerosol extinction coefficient at 355 and 532 nm (in Mm^{-1}), aerosol backscatter coefficient at 355, 532 and 1064 nm (in $Mm^{-1}\ sr^{-1}$), lidar ratio (LR), at 355 and 532 nm (in sr), aerosol extinction and backscatter-related Ångström exponent (355 nm/532 nm), water vapor mixing ratio (in $g\,kg^{-1}$) and relative humidity (%), as retrieved by Raman lidar measurements over Athens on 22 April 2010, between 01:30 UTC and 03:00 UTC (upper graph) and 20:00 UTC and 22:00 UTC (lower graph).

ACPD
13, 5315–5364, 2013

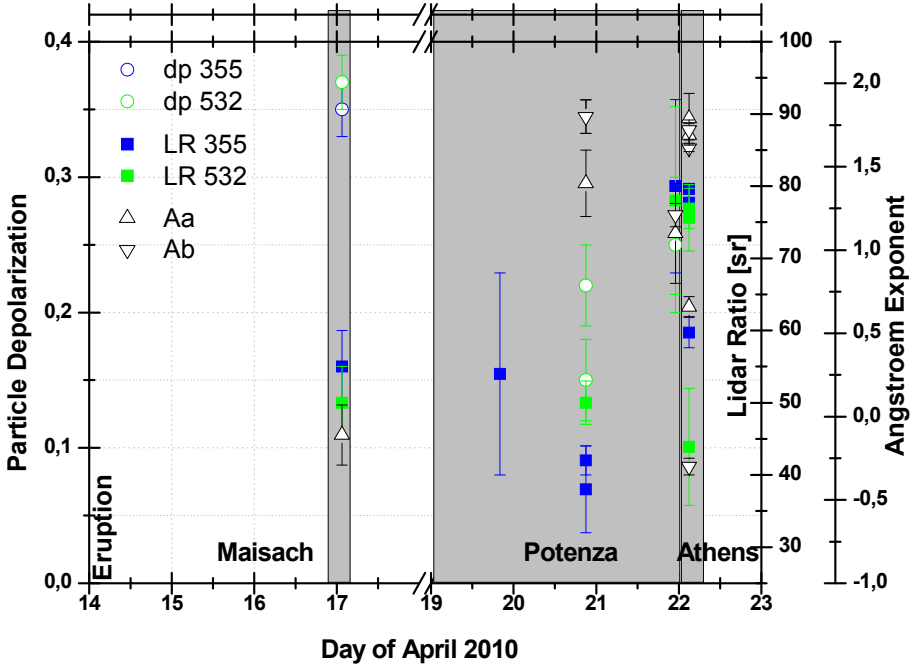

Fig. 12. Aerosol optical properties (depolarization ratio, LR, extinction and backscatter-related Ångström exponent) from various studies, inside volcanic aerosol layers, as obtained over Maisach, Germany (Gross et al., 2011), Potenza, Italy (Mona et al., 2011) and Athens, Greece (present study) from 17–23 April 2010.

ACPD
13, 5315–5364, 2013

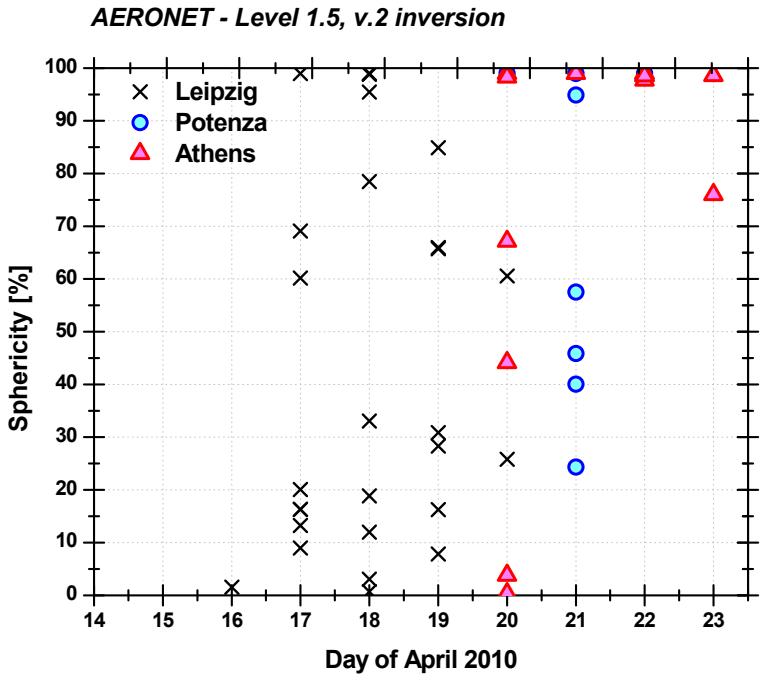

Fig. 13. Columnar aerosol sphericity values, obtained from the AERONET level 1.5 standard product, over Leipzig, Potenza and Athens, from 16–23 April 2010.

ACPD
13, 5315–5364, 2013

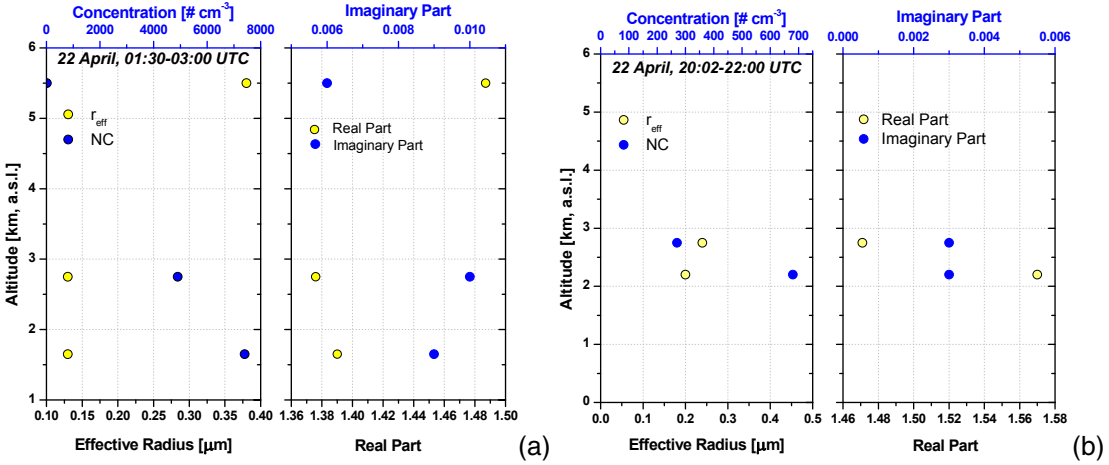

Fig. 14. Aerosol properties derived from lidar inversion code using NTUA Raman lidar data: mean effective radius, number concentration, and refractive index (real and imaginary part) between 0.6 and 6 km height, over Athens on 22 April 2010, **(a)** between 01:30 UTC and 03:00 UTC and **(b)** between 20:00 UTC and 22:00 UTC.

ACPD
13, 5315–5364, 2013